PURIFICATION OF CRUDE GLYCEROL BY A COMBINATION OF PHYSICO-CHEMICAL TREATMENT AND SEMI-CONTINUOUS MEMBRANE FILTRATION PROCESSES

A Thesis Submitted to the
College of Graduate and Postdoctoral Studies
In Partial Fulfillment of the Requirements
For the Degree of Master of Science (M.Sc.)
In the Department of Chemical and Biological Engineering
University of Saskatchewan
Saskatoon

By

Chol Ghai Chol

PERMISSION TO USE AND DISCLAIMER STATEMENT

In presenting this thesis in partial fulfillment of the requirements of the degree of Master of Science (M.Sc.) at the University of Saskatchewan, I agree that the Libraries at this institution may make it freely available for inspection. I further agree that the permission for copying of this thesis in any manner, in part or as a whole, for scholarly purposes may be done with granted written permission from the supervising professor(s), or in their absence, by the Head of the Department or the Dean of the College in or to which this work was done or submitted. It is to be understood that any copying, publication or use of this thesis or parts thereof for financial gain shall not be allowed without the express written permission from the author. It is also to be understood that due recognition shall be given to the author and to the University of Saskatchewan in any scholarly use that may be made of any material or part(s) of this thesis.

Disclaimer: The names of Milligan Biofuels, MITACS and Saskatchewan Ministry of Agriculture were mentioned to meet the degree requirements at the University of Saskatchewan. References in this thesis to any specific commercial product or process by any trade name, manufacturer, trademark or otherwise, does not constitute or imply its endorsement, recommendation or favouring by the University of Saskatchewan. The views or opinions expressed herein by the author do not state or reflect those of the University of Saskatchewan and shall not be used for any advertisement or endorsement purposes. Requests for permission to copy and/or make other uses of materials in this thesis in whole or in part should be addressed to one of the following:

Head of the Department of Chemical and Biological Engineering
University of Saskatchewan
57 Campus Dr.
Saskatoon SK, S7N 5A9 Canada

Dean
College of Graduate and Postdoctoral Studies
University of Saskatchewan
116 Thorvaldsen Building, 110 Science Place
Saskatoon, SK, S7N 5C9 Canada

ABSTRACT

Crude glycerol is being increasingly produced in large quantities industrially as a result of increasing biodiesel production and it poses a disposal challenge as it is of little economic value. When purified however it has economic value and a lot of uses including being valorized into fuel additives such as solketal ($C_6H_{12}O_3$) and glycerol carbonate ($C_4H_6O_4$). The purpose of this research therefore was to purify glycerol to technical grade (95 wt%) in the most economically feasible way. In this work, crude glycerol was purified by combined techniques of physico-chemical treatment and semi-continuous membrane filtration using tubular ceramic ultrafiltration and spiral wound polymeric nanofiltration membranes. Three parameters – temperature, pressure, and flow rate - were studied to observe their effects on membrane ultrafiltration of treated glycerol to optimize glycerol purity. A maximum glycerol purity of 93.7 wt% was obtained from purification of crude glycerol of 40 wt% original purity after physico-chemical treatment and membrane filtration using a 5 kDa ultrafiltration membrane at the temperature, pressure, and flow rate of 50°C, 690 kPa g, and 50 mL/min, respectively. Most of the purification occurred during physicochemical treatment. Nanofiltration of a simulated glycerol mixture at varying flow rates and salt contents produced a glycerol purity in the range 96 - 100 wt% up from 94 wt% purity glycerol. Nanofiltration of treated glycerol under various flow rates and relatively constant pressure and salt content at room temperature produced the highest glycerol purities of 97.2 and 94.9 wt% at 80 and 125 mL/min flow rates respectively, both purities of which are of technical grade. Techno-economic analysis of glycerol purified by combined physico-chemical and ultrafiltration techniques based on a scenario where all the purified glycerol was converted to value added chemicals – solketal and glycerol carbonate – has shown that the glycerol purification process is economically feasible with more than 100% return in net present value on capital.

ACKNOWLEDGEMENTS

I wish to acknowledge the following people for their steadfast and unwavering support during my pursuit of Master of Science (M.Sc.) degree in Chemical Engineering. My supervisor Dr. Ajay K. Dalai for his great supervision, mentorship and critical guidance and review of my work throughout my studies from start to finish. My Academic Advisory Committee members Dr. Hui Wang and Dr. Lifeng Zhang for their guidance, feedback and instructions during the course of my academic pursuit of this degree. I also acknowledge my external examiner Dr. Lee Wilson for his great examining work.

I acknowledge Milligan Biofuels for providing me with crude and pure glycerol samples for my experimental investigations. I also acknowledge MITACS, Saskatchewan Ministry of Agriculture, the Department of Chemical and Biological Engineering and the University of Saskatchewan for providing me with financial support and funding during the course of this work. I want to acknowledge research associate Dr. Ravi Dhabhai for his extraordinary assistance during my experimental investigations including in fixing the membrane setup, and also for his help during data collection and analysis and also in proofreading and providing comments for my work.

I want to thank RLee Prokoshyn for building the membrane setup used in this work, and for fixing it and helping to troubleshoot any repair problems with it every time. Also thanks to technicians Heli Eunike and Richard Blondin for their help during my instrument analysis of my samples including in selecting the most perfect technique and/or apparatus to use. And last but not least, I want to acknowledge all the members of Dr. Dalai's Catalysis and Chemical Reaction Engineering Laboratories (CCREL) group for the help and support they have provided during the course of my studies.

PERMISSION TO REPRODUCE

Parts of this work were reproduced from a paper published by this author in the Journal of Fuel Processing Technology of Elsevier. The said parts include parts of abstract, introduction, results and discussion and conclusion. This author has written to the Journal and is awaiting permission, which when received will be in Appendix A of this work.

DEDICATION

To my mum, my maternal uncle Deng Ajang Awai and my families on mum's and dad's side. To the memories of my dad and my grandmothers. To Jesuit Refugee Service (JRS). To World University Service of Canada (WUSC).

TABLE OF CONTENTS

LIST OF TABLES

LIST OF FIGURES

NOMENCLATURE

A – membrane area (m^2)

AC – activated carbon

ANOVA – analysis of variance

C – concentration (wt% or g/m^3)

CAPEX – capital expense

CCD – Central Composite Design

Da/kDa – Dalton/kiloDalton

DBEB – discounted break-even period

DMF – dimethylformamide

ED – electrodialysis

ETBE – ethyl tert-butyl ether FAME – fatty acid methyl esters

FFAs/SFAs – free fatty acids/saponified fatty acids

FR – flow rate (kg/s or m^3/s)

FR – flux recovery (%)

GAC – granular-activated carbon

HHV – high heating values (MJ/kg)

J – flux (g/m^2s)

K – Darcy permeability coefficient (m^3/m^2s Pa)

k_m – membrane resistance coefficient (m^{-1})

LCDs – limiting current densities (A/m^2)

LHV – low heating value (MJ/kg)

LLE – liquid-liquid equilibrium

MONG – matter organic non-glycerol

MTBE – methyl tert-butyl ether

MWCNTs – multiwall carbon nanotubes

MWCO – molecular weight cut-off

NCSR – nanocomposite solvent resistance

NF – nanofiltration

NPV/NPW – net present value/worth

NRTL – non-random two liquid

OPEX – Operating expense

P – pressure (kPa) or permeability (m/s)

PAC – powder-activated carbon

PFD – process flow diagram

PI – polyimide

Q – flow rate (kg/s or m^3/s)

R – retention (%)

Re – Reynolds number

RO – reverse osmosis

RSM – response surface methodology

T – temperature (^{o}C or K)

TMP – transmembrane pressure (kPa)

UF – ultrafiltration

UNIQUAC – quasi-chemical model

ΔP – pressure differential (kPa)

Δx – membrane thickness (m)

μ - dynamic viscosity ($kgm^{-1}s^{-1}$)

2FI – two-factor interaction

η – viscosity (cP)

σ - reflection co-efficient (-)

1 INTRODUCTION

Glycerol is the an organic co-product of the biodiesel production process produced in significant quantities, about 10 wt% of the total biodiesel (Hajek et al., 2010). Glycerol ($C_3H_8O_3$) is a trivalent alcohol that is also known as glycerine, 1,2,3-propanetriol, glyceritol, glycyl alcohol, or 1,2,3-trihydroxypropane (Ardi et al., 2015; Dhabhai et al., 2016). Homogeneous catalytic transesterification is the major source for most crude glycerol production (Dhabhai et al., 2016). The transesterification reaction is shown in the schematic in Figure 1-1 (Tan et al., 2013).

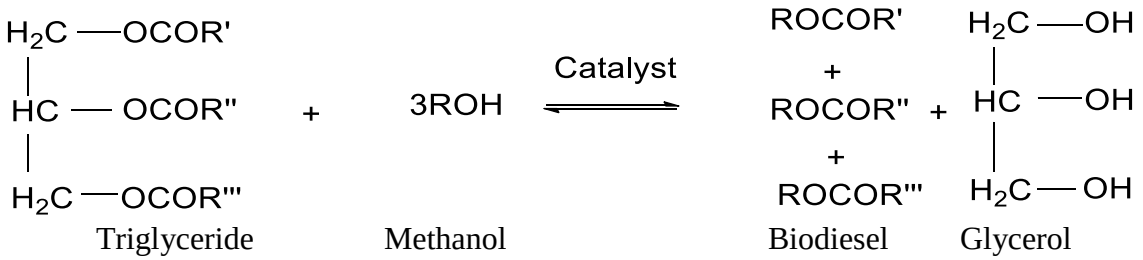

Figure 1-1 Schematic for transesterification reaction

Where R', R" and R"' are long chains of carbon and hydrogen atoms, also called fatty acid chains

Two phases are formed during biodiesel production following transesterification and separation of excess alcohol (Hajek et al., 2010). The upper phase is the ester phase which contains biodiesel while the lower phase is glycerol and consists of glycerol, water, organic and inorganic salts, tiny quantities of esters and alcohol, trace amounts of glycerides and vegetable colours (Hajek et al., 2010). The exact composition of the bottom crude glycerol phase depends on the transesterification method used to produce glycerol and biodiesel; the catalyst used in the said process; the process efficiency; the biodiesel separation conditions and the recovery efficiency of biodiesel; the presence of other impurities in the feedstock; and recovery of solvent and catalyst (Dhabhai et al., 2016; Yang et al., 2012; Hajek et al., 2010). But glycerol composition ranges from 30 to 60 wt% (Hajek et al., 2010; Yang et al., 2012). Most biodiesel production processes use methanol and homogeneous alkaline catalysts such as sodium or potassium methoxide or

hydroxide. Accordingly, crude glycerol contains impurities such as inorganic salts, matter organic non-glycerol (MONG) and water (Yang et al., 2012). MONG consists of fatty acid methyl esters (FAME), tri-, di- and mono-glycerides, several types of free fatty acids (FFAs), and methanol or ethanol (Dhabhai et al., 2016). (Hajek et al., 2010).

Glycerol can also be produced from saponification of triglycerides from vegetable oils or animal fats to form soaps (Hajek et al., 2010; Tan et al., 2013). During this process, triglycerides are converted into fatty acid salts (soap) and glycerol by use of alkaline hydroxides (Hajek et al., 201; Tan et al., 2013). Table 1-1 shows the composition of crude glycerol produced by different processes, according to existing literature.

Table 1-1 Different compositions of crude glycerol produced by different processes (Isahak et al., 2016; Isahak et al., 2010)

Component	**Transesterification (wt%)**	**Saponification (wt%)**	**Hydrolysis (wt%)**
Glycerol	30-60	83-84	88-90
Ash	10-19	8.5-9.5	0.7-1.0
Water	≤10	6-7	8-9
MONG (Matter Organic Non-Glycerol)	≤40	3-4	0.7-1.0
Trimethylene glycol	1	0.1	0.2

Glycerol is a colourless, odourless, and viscous liquid at room temperature and is biodegradable, hygroscopic and non-toxic. It is a liquid that contains three hydrophilic hydroxyl groups that make it hygroscopic and soluble in water (Perry et al., 1997; Brady et al., 1990). Glycerol is renewable and biodegradable and is produced by the green refining industries, making it great for the environment and can be an alternative to fossil fuels (Rahmat et al., 2010). If combined with biodiesel, glycerol as an alternative energy source would have additional advantages in energy integration (Metzger et al., 2007). It is also such a versatile building block it

has thousands of uses including in the food, cosmetic, chemical and pharmaceutical industries (Ardi et al., 2015; Dhabhai et al., 2016; Werpy et al., 2004; Shen et al., 2014; Teng et al., 2014).

Glycerol is totally miscible in a lot of substances including alcohols, ethylene glycol, propylene glycol, trimethylene glycol monoethyl ether and phenol (Lopes et al., 1999; Chung et al., 2007).

Glycerol is very viscous and remains a viscous liquid but aqueous glycerol solutions at different concentrations do have low viscosity (Miner et al., 1953). Table 1-2 shows the viscosities and high heating values (HHV) of crude glycerol produced from different feedstocks.

Table 1-2 Average viscosities and heats of combustion of crude glycerol from different feedstocks (Thompson et al., 2006)

Feedstock	Ida Gold	Pack Gold	Rapeseed	Canola	Soybean	Cramble
Viscosity of crude glycerol at 40^{o}C (cP)	8.80	8.67	8.50	8.46	8.65	8.50
HHV of crude glycerol (MJ/kg)	18.60	19.428	19.721	20.510	19.627	19.472

*Ida Gold and Pack Gold are mustard oilseed varieties

The calorific value of glycerol is determined by the raw material used to produce it. Compared to fossil fuels, glycerol has twice their calorific values but comparable to the heats of combustion of most biomasses (Stelmachowski et al., 2011). Table 1-3 lists the values for the most important physical and chemical properties of glycerol.

Table 1-3 Physical and chemical properties of glycerol

Property	**Units**	**Value (Morrison et al; Pagliaro & Rossi et al, 2007; OECD-SIDS)**
Molecular formula		$C_3H_5(OH)_3$ or $C_3H_8O_3$
Molar mass	g/mol	92.0 – 92.09
Relative density	Kg/m^3	1260 – 1261
Viscosity	Pa s	1.41 – 1.50
Melting point	^oC	18.0 – 18.2
Boiling point (at 101.3 kPa)	^oC	290
Flash point	^oC	160 – 177
Specific heat (at 25^oC)	kJ/kg	2435
Heat of vaporization	kJ/kmol	82.12
Thermal conductivity	Wj(mK)	0.28
Heat of formation	kJ/mol	667.8
Surface tension	mN/m	63.4 – 64.0
pH (solution)		7
Auto flammability	^oC	393

Purification of glycerol increases its economic and applicable value and makes biodiesel production more viable (Dhabhai et al., 2016). Pure glycerol is a renewable commodity and feedstock for biorefineries (food, chemical, and pharmaceutical industries) and can be used in the production of fuels or fuel additives (Ardi et al., 2015; Dhabhai et al., 2016). Glycerol purity is defined by its grade – 95% purity glycerol is classified as technical grade; 96-99% purity glycerol as USP grade glycerol; and 99.7% purity glycerol as Kosher glycerol (Ciriminna et al., 2014). Technical grade glycerol is used as a building block in chemicals but is not used in food production or drug formulation (Ciriminna et al., 2014). USP (United States Pharmacopeia) grade glycerol is

employable in production of foods and pharmaceuticals while Kosher glycerol is suitable for use in Kosher foods production (Ciriminna et al., 2014).

Due to glycerol overproduction resulting in large surpluses of glycerol formed as by-product of the biodiesel industry, opportunities have emerged for valorizing glycerol into value-added chemicals, which can make biodiesel commercially more viable (Fan et al., 2010). Glycerol can be valorized into value-added commodity chemicals and fuels through selective catalytic processes such as oxidation, hydrogenation, selective etherification and carboxylation among other processes (Fan et al., 2010).

Glycerol valorization by selective etherification can give rise to valuable fuel additives or solvents with appropriate properties such as tert-butyl ethers, which are potentially utilizable as diesel fuel additives in gasoline and as an alternative to methyl tert-butyl ether (MTBE) and ethyl tert-butyl ether (ETBE) (Clacens, 2002; Kunieda et al., 2002).

Carboxylation of glycerol produces glycerol carbonate, which has received plenty of attention in the chemical industry of late because it can be utilized in new polymeric materials as a cheap source (Vieville et al., 1998; Dibenedetto et al., 2006; Aresta et al., 2006). Glycerol carboxylation reaction is as shown in Figure 1-2 (Sonnati et al., 2013).

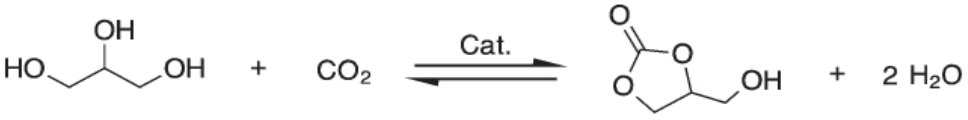

Glycerol Glycerol carbonate

Figure 1-2 Synthesis of glycerol carbonate from glycerol and carbon dioxide

Glycerol acetalisation with acetone can also be carried out over different sulfonic acid-modified mesostructured silicas for synthesis of solketal (2,2-dimethyl-1,3-dioxolan-4-methanol) as shown in the schematic in Figure 1-3 (Vicente et al., 2010).

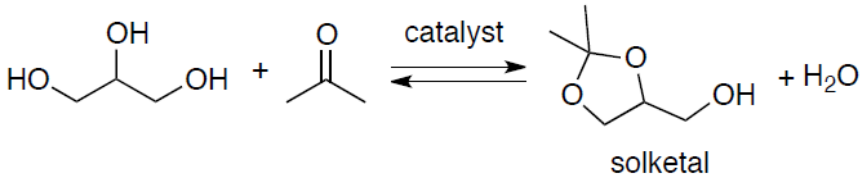

Figure 1-3 Solketal synthesis by glycerol condensation with acetone

1.1 Knowledge Gaps, Hypothesis and Research Objectives

Based on the above background and the additional literature discussed in chapter 2, the following knowledge gaps have been identified and the subsequent hypotheses and objectives formulated.

1.1.1 Knowledge Gaps

1. The combination of physico-chemical treatment and membrane filtration has not been thoroughly investigated for crude glycerol purification.

2. Glycerol purification has not been done using tubular membranes operated in semi-continuous mode.

3. The techno-economic analysis of crude glycerol purification by a combination of physico-chemical treatment steps and semi-continuous membrane filtration processes has not been investigated.

1.1.2 Hypothesis

1. Physico-chemical treatment can separate fatty acids, soaps, fatty acid methyl ester (FAME), and esters by saponification, acidification, and solvent extraction unit operations.

2. Given their small sizes (including in the range 1-5 kDa MWCO or 1-100nm), membranes can purify crude glycerol to technical grade (95 wt%) following initial physico-chemical treatment by separating organic macromolecules, colloids, residual MONG and salts from glycerol.

3. Given the fact that some membranes are relatively inexpensive, it can be economically feasible to incorporate semi-continuous membrane filtration into sequential treatment of crude glycerol by physico-chemical steps to obtain technical grade glycerol.

1.1.3 Objectives

To the best of this author's knowledge, no previous work has been done on glycerol purification using tubular membranes operated in semi-continuous mode in combination with physico-chemical processes. The following objectives have thus been formulated for this work.

1. To optimize glycerol purification using:

    a) Tubular ceramic ultrafiltration membranes in semi continuous mode in combination with physico-chemical processes by varying temperature, flow rate and pressure for membrane filtration

        (i) Temperature was varied from 25 to 60°C

        (ii) Flow rate was varied from 50 to 200 mL/min

        (iii) Pressure was varied from 345 to 1380 kPa

    b) Spiral wound polymeric nanofiltration membranes by varying salt content and flow rate.

        (i) Salt content was varied from 3 wt% to 6 wt% during nanofiltration

        (ii) Flow rate was varied from 50 to 200 mL/min

2. To carry out techno-economic analysis of the optimized membrane purification of glycerol to determine the economic feasibility of the process at industrial level.

2 LITERATURE REVIEW

This section presents literature on glycerol availability, purification processes and the membrane filtration technology.

2.1 Crude glycerol availability

Global glycerol market size was projected at 2.44 Mt and USD 1.64 billion in 2014 and is estimated to experience an annual growth above 6.5% from 2015 to 2022 (Radiant Insights Inc., 2017 https://www.radiantinsights.com/research/glycerol-market). A sizable chunk of this supply was and will be surplus, posing a problem of disposal, since crude glycerol is of little economic value and use due to the presence of inorganic salts and other impurities (Ciriminna et al., 2014). The crude glycerol price in 2014 was $240/tonne while for pure glycerol (USP grade), it was $900/tonne (Ciriminna et al., 2014).

2.2 Glycerol purification processes and technologies in literature

Various practical methods and techniques are used to recover and/or enrich glycerol produced by hydrolysis, saponification and transesterification reactions among other physico-chemical treatment processes (Addison et al., 2006). Treatment of glycerol produced from an alkaline catalyst starts with neutralization using a certain acid, a move that tends to efficiently remove alkaline matter including excess catalyst and lots of soap formed during transesterification using homogeneous catalysts (Addison et al., 2006). Neutralization using a strong to moderately strong mineral acid separates the reaction mixture into three phases using a strong or medium-strength mineral acid: the bottom catalyst phase, the middle neutralized glycerol and methanol phase, and the top free fatty acid phase (Addison et al., 2006). Hydrochloric or sulphuric acid is sometimes employed during re-neutralization, resulting in formation of sodium chloride or potassium sulfate salts respectively (Isahak et al, 2009). Choosing phosphoric acid for re-neutralization is however viewed as more environmentally friendly as it forms a phosphate salt

that is a popular choice as a fertilizer (Isahak et al., 2009). The acid amount and concentration used in neutralization have significant effects on the separation time and ease of removal free fatty acids and salts (Banavali et al, 2009).

To achieve high levels of purity considered safe for consumption glycerol by US Food and Drug Association (FDA), excess methanol in crude glycerol has to be removed, which is made possible through flash evaporation (Brockmann et al., 1987). This technique removes 100% of the methanol based on its boiling point (Brockmann et al., 1987).

Neutralization, ultrafiltration, vacuum distillation, ion exchange or a combination of any of these methods in a single or multi-stages have been deployed for glycerol purification. A combination of more than one method during glycerol purification, according to studies, produces high-purity glycerol of greater than 99.2% purity (Isahak et al., 2015). Purification can cost as low as 0.149 USD$/kg (Isahak et al., 2015). In purification of crude glycerol, vacuum distillation, ion exchange, membrane separation, and activated carbon adsorption are regarded as deep refining technologies (Ardi et al., 2015). Of these processes, vacuum distillation and ion exchange are energy- and cost-intensive processes for purifying glycerol resulting in high energy input requirement (Ardi et al., 2015). Furthermore, the salt content in crude glycerol originating from homogeneous catalytic processes usually ranges from 5-7 %, making the conventional purification techniques costly (Yang et al., 2012).

Membrane filtration is an emerging technology in glycerol purification and is highly appealing because of its simple operability, low energy requirement and therefore low cost, good purification performance (>90 wt% glycerol output) and environmental friendliness (Wang et al., 2011; Singh et al., 2015). Membrane performance is dependent on several factors including membrane material and porosity, feed temperature, pH, trans-membrane pressure, tangential

velocity, and interaction between membrane and feed (Wang et al., 2011; Singh et al., 2015). Caking of membrane material and fouling remain real challenges during membrane filtration (Wang et al., 2011; Singh et al., 2015). Ceramic membranes are emerging as a good alternative to conventional polymeric membranes because of their great thermal, chemical, and mechanical stability properties, higher permeability, and easy cleaning process (Luo et al., 2016; Le et al., 2016). Among the finishing steps, activated carbon adsorption removes colour in crude glycerol and removes some free fatty acids (lauric and myristic acids) by adsorbing them along with other molecular compounds (Ardi et al., 2015; Dhabhai et al., 2016; Luo et al., 2016).

Below is a discussion of processes in literature that have been used to purify glycerol. Ooi et al. (2001) subjected eight samples of residual glycerol from one batch to chemical and physical treatment to recover glycerol content of 51.4 wt% purity. Contreras-Andrade et al. (2015) purified raw glycerol from the transesterification process in the biodiesel industry by sequential extraction with organic solvents petroleum ether and toluene followed by decolorization using activated coal to obtain a final glycerol of 99.2%. Hunsom et al. (2013) performed a comparative study of crude glycerol enrichment using solvent extraction and adsorption at a laboratory temperature of 30^{o}C by investigating the effects of parameters such as glycerol, ash and contaminant contents and colour to obtain the highest purity of 99.1% and 99.1% colour removal, which were the results of the combined process of n-C_3H_7OH extraction at a ratio of 2:1 along with activated carbon adsorption. A cost analysis of the crude glycerol enrichment was carried out and it showed enrichment by the combined process using n-C_3H_7OH extraction and adsorption to be 28.6% more expensive than that using chemical extraction with $C_4H_{10}O$ and adsorption (Hunsom et al., 2013). Manosak et al. (2011) refined crude glycerol derived from waste used-oil biodiesel production plant that is ester-based by sequential stage physico-chemical using sequential acidification to a

pH of 2.5 with phosphoric acid, phase separation and extraction with C_3H_7OH at a ratio of 2:1 v/v solvent to crude glycerol followed by adsorption with commercially activated carbon at a 200 g/l dosage to obtain 95.74 wt% highest glycerol purity and 99.7% colour reduction.

Hunsom et al. (2013) also performed adsorptive purification of crude glycerol obtained from transesterification of used-oil and methanol in a biodiesel plant using KOH-impregnated AC carbonized at 800^oC for suitable surface properties to enhance pre-treated crude glycerol purity to 93.0 wt% with an AC dose of 67 g/L, an adsorption time of 2 h and a shaking rate of 250 rpm. Javani et al. (2012) acidified already saponified crude glycerol to pH 9.67 with phosphoric acid followed by acidification to pH 4.67 to produce high quality potassium phosphate and glycerol of purity 96.08%. Cai et al. (2013) purified original crude glycerol from biodiesel production by conducting a combined chemical and physical treatment using repeated acidification cycles of liquid phase to the desired pH value using 5.85% H_3PO_4 with the mixture kept at 70^oC for 60 minutes to make phase separation possible to obtain a glycerol-rich middle phase with a yield of 81.2%. Subsequent reaction of the glycerol phase with 0.03% sodium oxalate at 80^oC for 30 minutes resulted in 19.8% impurity removal before further purification via vacuum distillation and decolorization using two rounds of 2% of activated carbon at 80^oC to obtain a final glycerol of 98.1% purity (Cai et al., 2013).

Peyravi et al. (2015) developed and utilized nanocomposite solvent resistance (NCSR) membranes for separating organic biodiesel rich phase produced from alkaline catalyst transesterification of canola oil by filtering it via dead-end filtration mode at 5 bar pressure and 25^oC temperature, which resulted in increased glycerol removal from biodiesel with increasing MWCNTs content in the modified PI membrane up to 100% for M_3 membrane with no major changes in methyl ester flux, a result that was attributed to smaller surface pore size and a higher

membrane porosity following bulk modification. Wang et al. (2009) developed a ceramic membrane separation process for purifying biodiesel with the intent to reduce the significant amount of water used in biodiesel conventional water washing by micro-filtering crude biodiesel using ceramic membranes of pore size 0.6, 0.2 and 0.1 µm to remove free glycerol, catalyst and residual soap at transmembrane pressure of 0.15 MPa, temperature of 60^{o}C and membrane module flux maintained at 300 $Lm^{-2}h^{-1}$ at volumetric concentrated ratio of 4 for final free glycerol residue in biodiesel permeate estimated at 0.0108 wt% by water extraction. This ceramic membrane technology thus represents a potentially huge process in terms of environmental friendliness for biodiesel purification.

Methanol was found to be the right solvent for cleaning the membrane after microfiltration as it dissolves both free glycerol and soap (Wang et al., 2009). As an alternative to the water wash purification method for biodiesel enrichment, Saleh et al. (2011) designed and utilized a ceramic membrane separation system for glycerol removal from crude FAME (biodiesel) during the production of biodiesel. Ceramic membranes of the ultrafiltration (0.05µm) and microfiltration (0.2µm) types were run at varying operating temperatures (0, 5 and 25^{o}C) with all the runs separating glycerol from crude biodiesel and the 3-hour run using an ultrafiltration membrane at 25^{o}C meeting the international standards with a concentration factor higher than 1.6 (Saleh et al., 2011). Atadashi et al. (2015) purified crude biodiesel by ultra-filtering it using multichannel tubular membrane of 0.05 µm pore size to obtain best retention coefficients (%R) of 97.5% for free glycerol and 96.6% soap while the resultant biodiesel met the standards specified in ASTMD6751-03 and EN14214 standards with no wastewater generation. Vadthya et al. (2015) used commercial AMI-7001 and CMI-7000 ion exchange membranes along with limiting current densities (LCDs) to perform electrodialysis (ED) and separated over 95% of Na_2SO_4 from crude

glycerol thus demonstrating electrodialysis as a simple and cost-effective technology crucial in adding value to biodiesel via by-product recovery.

Isahak et al. (2010) purified crude glycerol produced from homogeneous catalyst (NaOH) and crude glycerol from heterogeneous catalysis transesterification of RBD palm oil using KOH/Al_2O_3 by neutralization, microfiltration and ion exchange resins techniques with the resultant glycerol deemed comparable to the commercially pure glycerol when gauged by viscosity, pH value, free fatty acid value, moisture content and density. In another work, Isahak et al. (2016) investigated the purification of crude glycerol co-product of transesterification by employing the methods of neutralization and microfiltration with 0.45μm membrane before free salt and catalyst ions remaining in glycerol were then removed by ion exchange process using two types of Amberlite resins to produce high quality glycerol of 99.4 wt% purity as confirmed by FTIR, USP and ASTM methods. A simulation of the process using P2 and P5 simulation processes of the Super-Pro-Designer 7.0 software which allows for scaling up gave glycerol purities of 98.35 and 99.27 wt% respectively using several combination purification steps, which were comparably similar (Isahak et al., 2016).

Dhabhai et al. (2016) investigated crude glycerol purification by a sequential procedure consisting of saponification, acidification, neutralization, membrane filtration, solvent extraction and activated charcoal adsorption with membrane filtration at 60^{o}C and 350 kPa pressure using 1 kDa membrane followed by evaporation of methanol solvent and water and treatment with activated carbon producing the highest glycerol purity of 97.5 wt% with acid value below 1.1 wt% and free fatty acid (FFA) content less than 0.6 wt%. In their work, Sadhukhan et al. (2016) applied novel purification sequential steps using acidification, neutralization, solvent extraction,

decolourization and membrane pressure filtration with optimum conditions of pH 3.26 and 0.933 gm adsorbent quantity with phosphoric acid (0.43 N) resulting in glycerol purity of 90.4%.

2.3 Membrane Filtration Technology

Membrane filtration technology has been in use for many decades because of its many technical and feasibility advantages (Van-der-Bruggen et al., 2002). The membrane field has made immense advancement potential because of membranes being economical, environmentally friendly, versatile and easy to use, hence great choices in many purification applications (Alyson et al., 2011). Membranes have many advantages including thorough particles and dispersed and emulsified oils removal; minimal footprint size; low weight and energy requirements; and high output rates (Bjame et al., 2002). All those pros coupled with less space requirements, moderate costs and easy operability make membranes great choices for purification (Jeffrey et al., 1997). Membrane processes with pressure as driving force include microfiltration (MF), ultrafiltration (UF), nanofiltration (NF) and reverse osmosis (RO) with MF and UF often serving to remove organic macromolecules, large colloids and microorganisms (Jeffrey et al., 1997). MF acts as a porous barrier to decrease turbidity and eliminate colloidal suspensions while UF has higher removal than MF and it operates at a higher pressure. Ultrafiltration rejects bacteria, microorganisms and large molecules such as proteins and large particles. Reverse osmosis membranes reject particles along with many species with low molecular weights such as salt ions and organics (Jeffrey et al., 1997).

Membrane processes are projected to be key components in biorefineries as they have low energy requirement and low chemical consumption among other pros (Ramaswamy et al., 2013). Fractionation in membranes is dependent on membrane pore size and its operating parameters (Ramaswamy et al., 2013). Macromolecules concentration in membranes is performed by

ultrafiltration; concentration of monosaccharides, multivalent inorganic ions and low-molecular weight material by nanofiltration; and salts removal by reverse osmosis (Cortinas et al., 2002; Gullon, et al., 2008; Persson, et al., 2010; Arora et al., 2010; Schild et al., 2010; Zeitoun et al., 2010; Leberknight et al., 2011). Multivalent metal ions are rejected by nanofiltration membranes and to a great degree by UF membranes (Kirbawy et al., 1987; Wallberg et al., 2003). UF membranes retain macromolecules of sizes 1- 20 nm while nanofiltration membranes have pore sizes smaller than UF but larger than RO membranes. (Cheryan et al., 1998).

2.3.1 Membrane materials

The mechanical and chemical stability of membranes in addition to separation characteristics are key parameters when selecting membranes for specific processes or applications (Ramaswamy et al., 2013). Mechanical and chemical stability of a membrane are measured by maximum pressure and temperature respectively that a membrane is able to withstand (Ramaswamy et al., 2013). Chemical stability is measured by a pH range and in terms of resistance to solvents (Ramaswamy et al., 2013). Membranes are made from various materials including polymers and ceramics with the latter having higher temperature and pH resistance while the former have higher maximum pressure (Ramaswamy et al., 2013). Ceramic membranes are manufactured from α-Al_2O_3 and TiO_2 whereas regular polymeric membranes are made of polysulfone, polyethersulfone, polyvinylidene fluoride and regenerated cellulose (Bjame et al., 2002).

Ceramic ultrafiltration membranes are microporous sieves that separate on the basis of size and speed of a particle through a tortuous path of the pore (Singh et al., 2013). Capillarity, adsorption and surface charge all play a part in separation (Scott, 1995). Ceramic membranes are pretty limited in their ability to exclude based on size though they can be made with a sharp pore size distribution either through sintering or by sol-gel processes (Singh et al., 2013). UF

membranes are produced by the sol-gel process with $\gamma - alumina\ and\ \alpha - alumina$ as the most common ceramic membrane materials (Singh et al., 2013). Zirconia, titania, silicon carbide and glass (silica) are also used. Ceramic microfilters have greater rigidity and can accommodate fluxes 5-7 times greater than asymmetric polymeric membranes can handle and require regular backwash with no damage to the membrane skin layer necessarily (Singh et al., 2013). Ceramic membranes also have high temperature applications while polymeric membranes are limited to temperatures below 90^0C (Singh et al., 2013). In addition, ceramic membrane materials have greater resistance to cleaning chemicals and steam-sterilizing and repeated autoclaving, making them suitable for biopharmaceutical processes (Singh et al., 2013). Ceramic membranes are also advantageous because of their longer life (up to 10 years) (Singh et al., 2013). Polymeric materials have a typical lifespan of one to two years for hydrophilic membranes and three to five years for hydrophobic membranes (Singh et al., 2013). Ceramic materials are however brittle and more expensive than polymer-based membranes (Singh et al., 2013). Typical ceramic membranes are as shown in Figure 2-1.

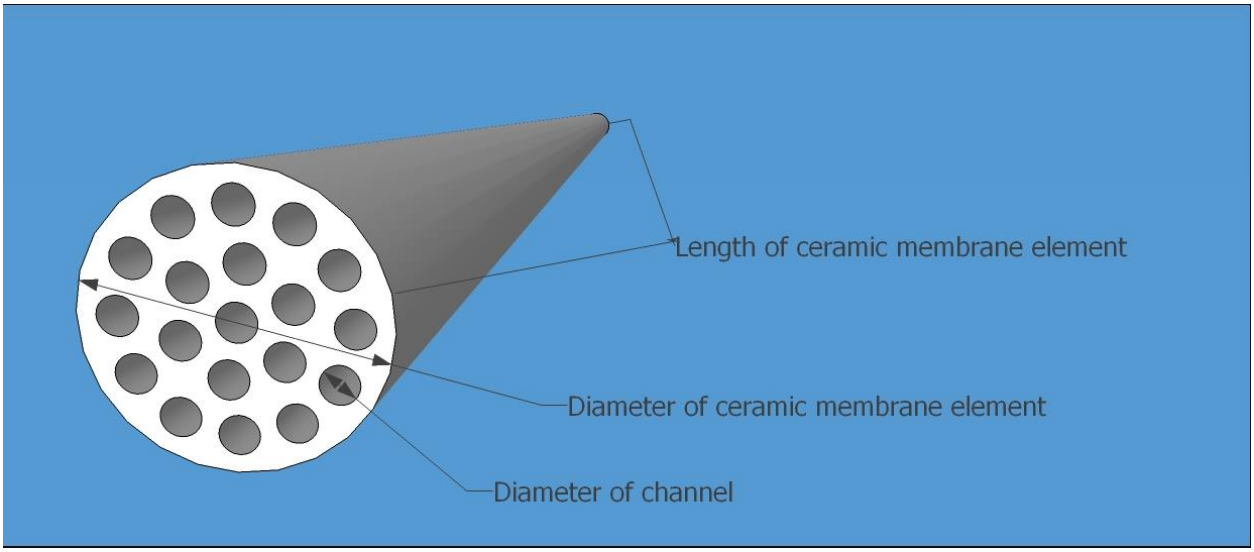

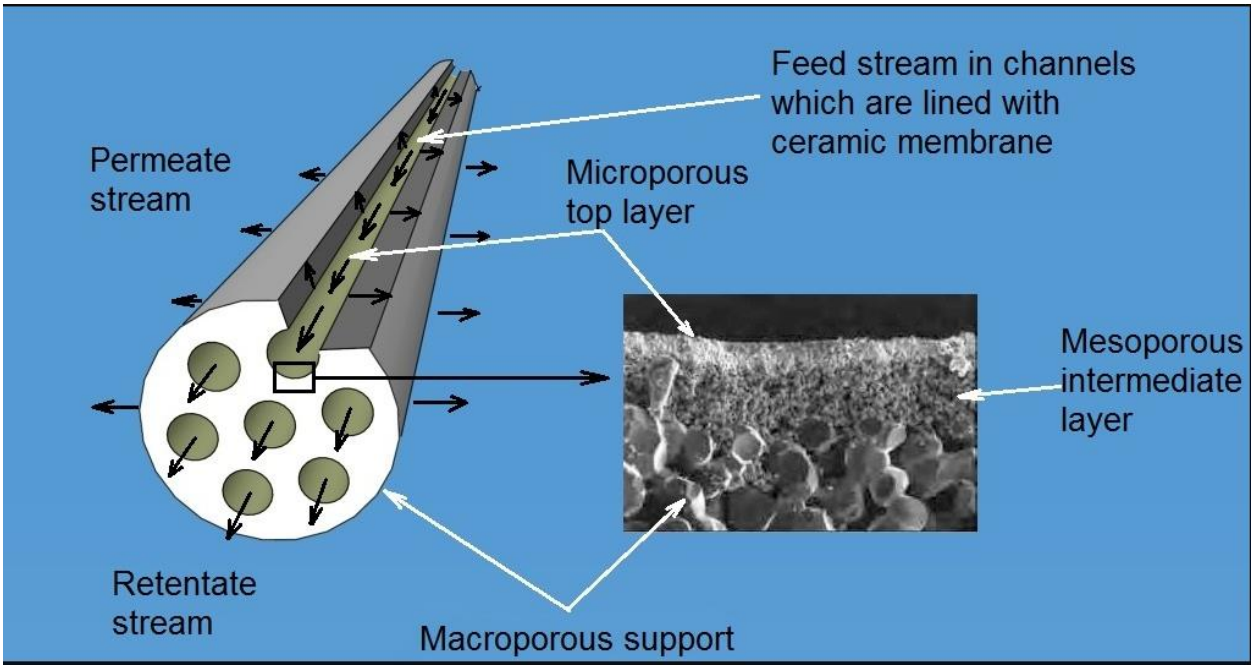

Figure 2-1 Typical ceramic membrane modules (Induceramic 2018)

2.3.2 Membrane-separation characteristics and transport

Membrane-separation entails simultaneous species retention and product flow through the semi-permeable membrane. High selectivity and flux of a membrane; good stability properties; defect-free production; reduced fouling; and environmental friendliness are ways in which membrane performance is measured (Singh et al., 2013). Membrane processes are continuous operations in steady-state with feed, product and reject streams (Strathmann et al., 2001; Lonsdale et al., 1982; Schafer et al., 2004).

No single membrane process is suitable for all fluid separation processes as separation depends on the nature of feed and membrane and product requirements as well as membrane design for the process and feed type (Table 2-1) (Singh et al., 2013).

Table 2-1 Classification of commercialized membrane processes (Singh et al., 2013)

Process	**Pore size**	**Driving force**	**Transport mechanism**
Ultrafiltration	0.001-0.05 μm	Pressure, 2-5 bar	Sieving
Nanofiltration	< 2.0nm	Pressure, 5-15 bar	Donnan exclusion or sorption-capillary flow

Membrane processes being rate processes mean the product quality depends on the relative rate of solvent and solute transport through membrane pores (Singh et al., 2013). Substances move through membranes by several mechanisms including diffusion and/or viscous flow (Singh et al., 2013). Solute transport properties through membranes are determined by membrane permeability and by the driving force (Singh et al., 2013). Under the influence of the driving force, the semi-permeable membrane allows passage of certain substances while rejecting others (Singh et al., 2013). Typical driving forces include pressure difference, concentration difference and electrical potential difference between feed and product sides even though flow factors such as axial solute diffusion, solvent longitudinal convection and flow-induced particle drag on membrane surface also play a part by affecting transport across membranes (Singh et al., 2013). The extent of driving force depends on the potential gradient across the membrane, which controls mass transfer between feed and product solutions (Singh et al., 2013). As they are steady-state processes, membrane processes have constant flow as soon as steady-state has been established unlike equilibrium processes such as distillation, evaporation and crystallization (Singh et al., 2013).

2.3.3 Membrane plant design and operation principles

The most important factors in membrane filtration plant design and operating principles are whether it should be single-staged or multi-staged, in batch or continuous mode operation and

what the module configuration used for the membrane should be (Jonsonn et al., Ramaswamy et al., 2013).

Single-stage membrane plants

Batch operation with a single-membrane module is the simplest membrane system commonly employed in laboratory experiments and it is ideal for treating small feed volumes (Singh et al., 2013). The feed pump and retentate valve regulate pressure and velocity in batch operation (Singh et al., 2013). Some of the retentate in a circulation loop can be internally circulated at high operating pressure and high cross-flow velocity (Ramaswamy et al., 2013).

Multistage membrane plants

A multistage membrane plant is made up of a number of feed-and-bleed stages connected in series and they are preferred in most continuous full-scale membrane plants (Singh et al., 2013). The concentration tends to be constant per stage and increases along with the process (Singh et al., 2013). The flux is usually higher in a multi-stage plant than in a single-stage similar plant, whose operating concentration is often the final (Singh et al., 2013). With increasing number of stages in a multi-staged plant, the flux begins to resemble that of a batch setup (Singh et al., 2013). The concentration of concentrate varies with stages in a membrane plant and determining the optimum number of such stages is an iterative process (Ramaswamy et al., 2013).

Membrane plant design is focused on membranes and modules and according to Brouckaert et al. and Wagner, the points discussed below are key in membrane plant design and operation (Brouckaert et al., 1999; Wagner et al., 2012).

2.3.4 Membrane filtration system and operating principles

Continuous cross-flow operation

Cross-flow membrane filtration is a continuous process in which the feed flows inside out with feed flowing in the tube side and permeate flowing radially out of walls of the tube (Singh et al., 2013). Most of the reject is sent back to the feed tank at high velocities of 4-5 m/s for recycling (Singh et al., 2013). Because of large internal diameters, the membrane elements are able to deal with feeds of up to 5% solid levels (Singh et al., 2013). This process is made possible by operation in turbulence to reduce solute cake build-up on the surface of the membrane (Singh et al., 2013). High turbulent cross-flow and large internal diameters eliminate the need for pre-filtration though periodic chemical cleaning is however desired to remove or dissolve strongly held accumulated particles not removed by backwash (Singh et al., 2013).

Semi-continuous dead-end filtration

This system operates in semi-continuous dead-end mode with in-between backwashing often in combination with air scouring either during filtration and/or backwashing cycle (Singh et al., 2013). The latter controls foulant build-up through particle removal from the membrane surface (Singh et al., 2013). Foulants not removed by backwashing are removed by chemical cleaning (Singh et al., 2013).

2.3.5 Membrane modules

Membranes have modules incorporated with five different modules designs being in the market, a choice of which depends on economic considerations and the module aspects from chemical engineering (Ramaswamy et al., 2013). The five different module designs available in the market are tubular modules, plate-and-frame modules, spiral-wound modules, hollow-fibre modules and rotating and vibrating modules (Cheryan et al., 1998; Mulder et al., 1991; Baker et al., 2004).

The key differences between these module configurations are in the price, footprint and risk of blockage of feed flow channel. Spiral-wound modules and hollow-fibre modules are less expensive and have small footprint (Ramaswamy et al., 2013). They are however susceptible to feed channel blockage and extensive pretreatment is therefore necessary (Ramaswamy et al., 2013). Tubular membranes have the largest footprint and highest energy requirement but have the advantage of less pretreatment needed (Ramaswamy et al., 2013). Plate-and-frame modules are best suited for treatment of viscous solutions though they have a downside of high capital cost (Ramaswamy et al., 2013). Rotating and vibration modules are employed in increasing shear forces at constant velocity, however, they are usually expensive (Ramaswamy et al., 2013).

Tubular modules tend to contain up to 18 tubular membranes with tube diameters ranging from 4 to 25nm (Ramaswamy et al., 2013). Plate-and-frame modules design is anchored in conventional filter press concept where the flat membranes and porous support discs or a fine-meshed spacer are joined together with a coarse spacer keeping the membranes apart while a continuous flow channel is formed (Ramaswamy et al., 2013). A spiral-wound module principally speaking is a plate-and-frame module with slight modifications so permeate is collected in a tube at its centre (Ramaswamy et al., 2013). A large number of membrane capillaries with diameters from 0.5 to 1.5mm make up a hollow-fibre module (Ramaswamy et al., 2013). Typical tubular and spiral-wound membrane modules are shown in Figure 2-2.

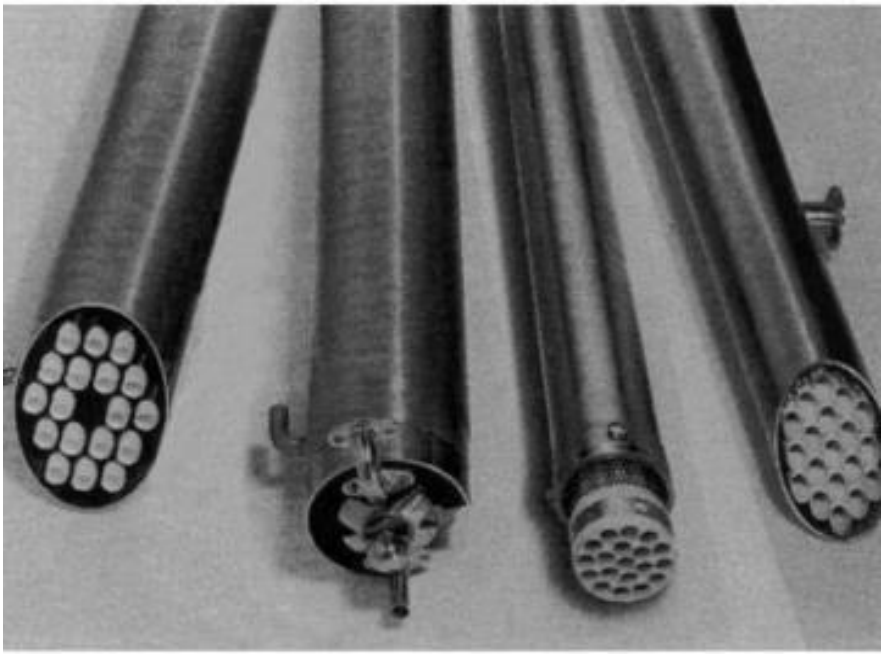

(a) Typical tubular filtration module (Singh et al., 2013)

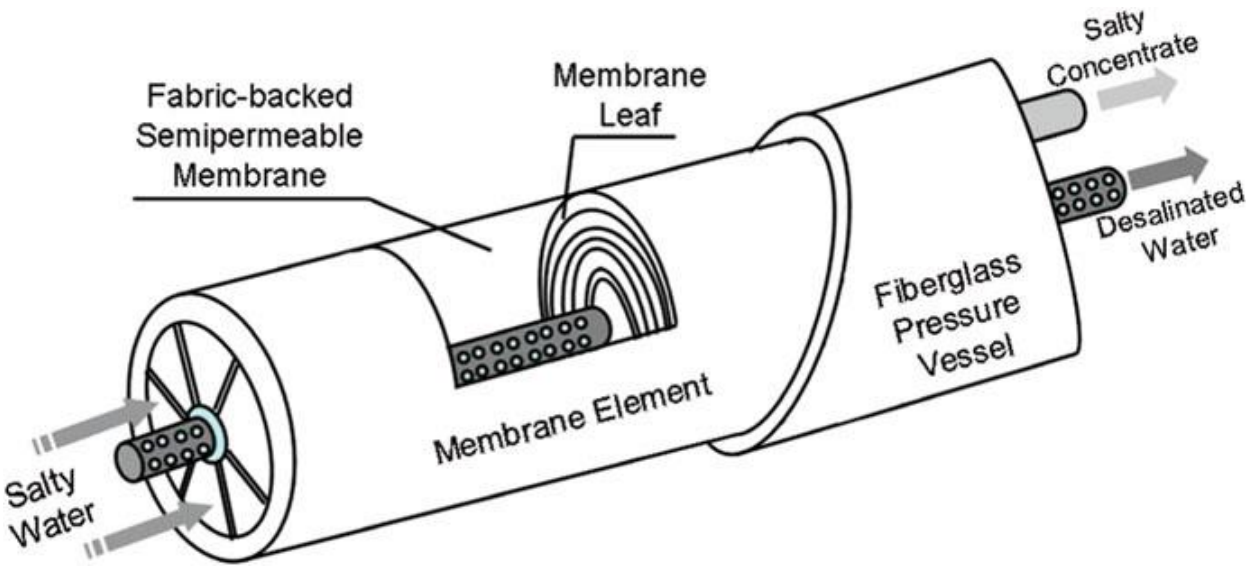

(b) Spiral wound membrane module (A. G. (Tony) Fane et al., 2011)

Figure 2-2 Tubular and spiral wound membrane modules

2.3.6 Process design for membranes

Process design optimization in a membrane plant is a trade-off between maximum flux, recovery and purity (Ramaswamy et al., 2013). Unfortunately maximum returns for recovery and purity are not compatible as much as a high flux is desirable as capital is inversely proportional to it while a high recovery is desired to ensure minimal raw material cost as well as a high purity product (Ramaswamy et al., 2013).

Retention

Membrane separation properties are specified in terms of retention (Ramaswamy et al., 2013). A membrane that retains all solutes has 100% retention while that with a retention of 0 solutes has none (Ramaswamy et al., 2013). Retention is dependent on operating conditions (Ramaswamy et al., 2013).

Recovery and purity

Recovery refers to the portion of a component in the feed that is collected as regular permeate product while product purity is dependent on the concentration of all compounds in the product side (Ramaswamy et al., 2013).

2.3.7 Effects of operating parameters for membrane filtration

Membrane performance and costs are dependent on a number of operating parameters and they require optimization in every specific application (Ramaswamy et al., 2013). Typical operating parameters include transmembrane pressure (TMP), cross-flow velocity, temperature and pH (Ramaswamy et al., 2013).

Effects of Pressure

Pressure in a membrane plant is measured at the inlet, p_{in}, and at the outlet, p_{out}, of the membrane module and on the permeate side, p_p (Ramaswamy et al., 2013). Transmembrane pressure provides driving force in UF and is generally the average pressure difference across the membrane (Singh et al., 2013). TMP regulation is done using a retentate valve, though in ceramic membranes it is regulated by a valve on the permeate side of the module (Ramaswamy et al., 2013). In the event there is no permeate valve, atmospheric pressure is taken to equal permeate-side pressure (Ramaswamy et al., 2013).

Effects of Cross-flow velocity

Cross-flow velocity is deployed to decrease concentration polarization and increase mass transfer (Gekas et al., 1987; van den Berg et al., 1989; Lipnizki et al., 2002). In the film theory, the fluid flow in the boundary layer adjacent to the membrane surface is taken to be laminar whereas fluid flow outside this layer is turbulent with complete solute mixing (Ramaswamy et al., 2013). At steady state, the convective solute transport in the boundary layer is equal to the permeate flow and the diffusive back transport of solute into the bulk solution (Ramaswamy et al., 2013).

Effects of Temperature

Increasing feed temperature results in three flux enhancing effects, namely: viscosity of the permeate decreases resulting in higher flux; lower viscosity of the solution on the feed side of the membrane improves the mass transfer coefficient, and the lower bulk solution viscosity reduces frictional pressure drop, leading to increased flux (Ramaswamy et al., 2013).

Effects of Solute Concentration

Membrane processes are limited in terms of feed solution concentration in that no membrane process is able to concentrate solutes to dryness (Ramaswamy et al., 2013). In NF, it is often the osmotic pressure of the concentrated solute that is limiting the process while in UF, it is rather the lower mass transfer rate of the higher molecular mass substances retained by these membranes, along with high viscosity (Ramaswamy et al., 2013). Flux decreases as the concentration is increased but generally the flux varies proportionally with the logarithm of the bulk concentration (Ramaswamy et al., 2013).

2.3.8 Membrane pretreatment, fouling and cleaning and sanitization

Pretreatment

The tendency of a solution to foul may be reduced by suitable pretreatments of the solution, whether the pretreatment processes are mechanical, thermal or chemical. Feed solution is often modified by pH adjustment and fibre or particle removal (Ramaswamy et al., 2013).

Cleaning and sanitization

Minimizing cleaning and successfully cleaning membranes are of paramount importance if a membrane process is to be implemented industrially; bench-scale tests are used for studying fouling behaviors of different membranes (Ramaswamy et al., 2013). Some of the measures for reducing fouling are determined by the actual fouling phenomena (Ramaswamy et al., 2013). Caking is lessened by operating below the critical flux and by backpulsing, pore blocking and adsorption, which is reduced by using hydrophilic membranes, and by adjusting pH (Carrere et al., 2001; Bacchin et al., 2005; Cortinas et al., 2002; Leberknight et al., 2011; Krawzcyk et al., 2011; Jonsson et al., 1998; Puro et al., 2010; Brinck et al., 2000). Regular and prompt membrane cleaning

requires restoring membrane performance by preventing fouling from worsening with long-term adverse effects (Singh et al., 2013). Membrane cleaning involves removal of foulants and scalants from the membrane elements to restore flux and retention (Singh et al., 2013).

Cleaning and developing cleaning procedures are a matter of trial-and-error but the following are the main chemical and physical methods of membrane cleaning (Singh et al., 2013):

(i) Chemical detergents and cleaners to solubilize or disperse foulants. The cleaning efficiency of chemicals improves with increasing temperature as the rate of chemical reaction doubles with every 10^{o}C rise in temperature.

(ii) Hydraulic energy as represented by high flow velocity in feed channels. Cleaning should be ideally done under turbulence (Reynolds number Re>2100) in tubular membranes. Foam balls may sometimes be used for scraping dirt off membrane surfaces (Singh et al., 2013).

2.3.9 Ultrafiltration

Ultrafiltration lies between nanofiltration and microfiltration on the filtration spectrum and separates species about 1-100nm in size (Wang et al., 2011). Classification of UF membranes is based on nominal molecular weight cut-off (MWCO) in the range 1-200kDa (Nguyen, 2016; Peters et al., 2010; Wang et al., 2011). Ultrafiltration is a pressure-driven membrane process that is operated at low pressure (up to 1000 kPa) because the osmotic pressure exerted by the high molecular weight solutes is termed negligent (Peter et al., 2010; Singh et al., 2013; Wang et al., 2011).

Ultrafiltration is used for concentration and separation largely depends on species size. Ultrafiltration happens in the cross-flow mode, splitting the feed into two product streams:

permeate or filtrate and membrane-side retentate (Mohanty, 2010). Species volume, type and amount present in a permeate depend on membrane characteristics, operating conditions and feed quality (Wang et al., 2010). Retentate composition is determined by what filters out along with permeate (Wang et al., 2010). Osmotic backpressure in ultrafiltration is typically low hence the low applied pressure used for generating permeate (Wang et al., 2010). Membrane permeate flux is directly proportional to the productivity of ultrafiltration processes (Wang et al., 2010). Permeate flux is affected by parameters such as: membrane properties, feed properties, trans-membrane pressure and system hydrodynamics (Mohanty et al., 2010). Flux declines with time likely due to surfactant adsorption on wall of pores, polarized buildup layer of concentrate at membrane surface or pore plugging (Wang et al., 2011).

Ultrafiltration membranes are porous with distinct and permanent porous network in which transport occurs (Wang et al., 2010). Retained species are several orders of magnitude greater than the permeated ones (Wang et al., 2010). Ultrafiltration membranes can remove bacteria and viruses and can separate macromolecules (sugars, proteins), colloidal silica and pyrogens (Singh et al., 2013).

Flow in the ultrafiltration membrane pores is described by Pouiseille flow (Ren et al., 2010). Water and other solutes of low molecular mass pass through membrane pores while the macromolecules are rejected (Wang et al., 2011).

Darcy's law governs ultrafiltration and occurs in three steps: Sieving, adsorption and cake formation (Hu et al., 2014). These mechanisms are crucial in understanding membrane performance (Hu et al., 2014). Sieving is the primary filtration mechanism where particles larger than the MWCO are retained at membrane surface while smaller ones like water pass through (Hu et al., 2014). It's to be noted however that particulate removal is not an ideal step function of the

MWCO as other membrane properties and membrane-particle interface interactions also play a role (Hu et al., 2014). Soluble substances can be excluded despite having smaller physical dimensions than the MWCO (Hu et al., 2014).

Adsorption plays a role in the primary stage of filtration when the membrane is clean, however, the adsorption capacity does get exhausted and ceases to be effective long-term as a filtration mechanism (Hu et al., 2014). Adsorbed materials have the capability to decrease the MWCO by decreasing pore size cavities throughout the membrane hence increasing their capability to retain smaller material through sieving (Hu et al., 2014). During the filtration process, a clean membrane accumulates particles at the surface due to sieving (Hu et al., 2014). The accumulated solids form a particulate cake that acts as a dynamic filtration medium whose capability is a function of time from caking and backwash processes (Hu et al., 2014).

2.3.10 Nanofiltration

Nanofiltration (NF) is a newer pressure-dependent membrane filtration mechanism for separating molecules from liquids (Manttari et al., 2013). Nanofiltration is defined in many ways according to cut-off, size and salt retention (Ramaswamy et al., 2013). On the basis of cut-off, molecules with molecular weights under 300 g/mol (Daltons) are separated from macromolecules (Manttari et al., 2013). Commercially available NF membranes range from 200 to 1000 g/mol molecular weight (Manttari et al., 2013). Based on size, they are defined in terms of the largest project of the molecule with the general cut-off being about 1 nm (Manttari et al., 2013). Here molecular stiffness plays a role in separation (Manttari et al., 2013). When defined in terms of salt retention on the basis of the principle of charge and size, nanofiltration membranes retain over 98% of magnesium sulfate and under 50% of sodium chloride and thus are able to separate multivalent ions from monovalent ions (Mantarri et al., 2013). In practice, nanofiltration is for

separating multivalent salts as the first stage of desalination or for separating small organic molecules into the retentate or from organic macromolecules into the permeate (Manttari et al., 2013).

Fundamental principles

Nanofiltration is similar to reverse osmosis and ultrafiltration (Manttari et al., 2013). Tight NF is believed to be dependent on solution diffusion and requires a high pressure and working pressure by taking into account the osmotic pressure gradient across membrane (Manttari et al., 2013). In NF, both diffusion and convection are taken into account to achieve separation successfully (Manttari et al., 2013).

The working pressures for nanofiltration could be above 10 bars (1 MPa) but in case the osmotic pressure of the solution is not high enough, pressures between 4 and 8 bars (400 to 800 kPa) are used (Manttari et al., 2013). Flux in NF depends naturally on the membrane's propensity to foul (Manttari et al., 2013).

Retention, fractionation and influence of filtration parameters

When it comes to fractionation in NF, many possibilities can be considered for example size can be a criterion for separation just like in UF (Manttari et al., 2013). Nanofiltration membranes retain 90% of the uncharged molecules above the molecular weight cut-off and therefore fractionating the small molecular particles (Manttari et al., 2013). Other than the dissolved molecules size compared to membrane pore sizes sometimes determine achievable retention (Manttari et al., 2013).

Filtration parameters have a huge effect on nanofiltration membrane's ability to retain solute components (Manttari et al., 2013). Due to solution-diffusion mechanism of tight NF

membranes, retention lessens with constant flux conditions at high concentrate concentration or temperature (Manttari et al., 2013). This is due to diffusion increasing with increasing concentration and temperature (Manttari et al., 2013). Solution pH affects charged species and membrane functional groups (Manttari et al., 2013). When both have the same sign at a certain pH, the charge electrostatic repulsion increases retention. Retention can enormously be changed by a small change in pH (Manttari et al., 2013).

Solute retention

Retention of any component can in theory be described using Spiegler and Kedem (1966) equation for dissolved component transport through membrane with the two driving forces of diffusion (first term) and convection (second term) being crucial (Manttari et al., 2013):

$$J_s = -P\Delta\frac{dc}{dx} + (1-\sigma)J_v \quad (2\text{-}1)$$

J_s is components flux through the membranes (g/m^2s), P is component permeability (m/s), c is concentration (g/m^3), x is membrane thickness (m), J_v is permeate flux and σ is reflection coefficient (-).

Retention of organic and inorganic components

Organic molecules are sieved out of feed because they of their larger sizes or other interaction mechanisms with the membrane such as polarity or charge, when it exists (Manttari et al., 2013). Pore size in nanofiltration is approximately 1 nm (200 to 300 g/mol) (Manttari et al., 2013). There are a lot of transport models available for describing transport and retention of inorganics (Manttari et al., 2013). Ion retentions is simulated using the extended Nernst-Planck equation (Manttari et al., 2013).

Membrane materials and properties

Nanofiltration membranes tend to be made of many layers of material, potentially up to four (Manttari et al., 2013). The support layer, often made of a fibre network, gives strength to membrane so it is able to withstand with no extra resistance to the final membrane (Manttari et al., 2013). The second membrane layer can be a microfiltration or an ultrafiltration membrane and often has a supporting function (Manttari et al., 2013). The separating layer can be made from interacting chemicals above transport or is modified out of the top layer (Manttari et al., 2013). The top layer in NF membranes gives the membrane its functional properties such as cut-off, hydrophilicity, charge and others (Ramaswamy et al., 2013).

Structure of NF membranes

NF membranes are made of organic polymers and sometimes ceramics (Manttari et al., 2013). Composite NF membranes typically consist of a polysulfone sublayer and a top polyamide layer (Manttari et al., 2013). Cutoffs are difficult to make for ceramics or metals but could be possible in the near future (Manttari et al., 2013). Ceramic materials could stand more heat and solvents and are thus ideal in separation of oils and fuels, for example (Manttari et al., 2013).

Hydrophilic and hydrophobic characteristics

Hydrophilic and hydrophobic behaviors of a membrane are very important in that the former membrane types are less fouling when dealing with water solutions while the latter types are important in the separation of oils and solvents (Manttari et al., 2013).

2.4 Activated carbon

Activated carbon is made from organic materials heated to very high temperatures (>700^{o}C) and pyrolized in environments that are oxygen-deprived (Hu et al., 2013). Activated

carbon is usable as either granular-activated carbon (GAC) or powder-activated carbon (PAC) (Hu et al., 2013). PAC (average particle size: 20-50μm) is added for purification and is removed through sedimentation or filtration (Hu et al., 2013). GAC (mean particle size: 0.5-3mm) is often employed for filtration as a fixed bed (Hu et al., 2013). GAC can be impregnatable with iron to remove arsenic, or with ammonium ions for increased adsorption capacity for anionic species, and with silver for disinfectioning properties (Hu et al., 2014).

2.4.1 Important factors in adsorption: surface area, pore size and background matrix

Surface area and pore size are key factors that determine available number of adsorption sites for adsorbates (Hu et al., 2013). There is generally an inverse relationship between adsorption and surface area and pore size (Hu et al., 2013). Adsorption can be limited by steric effects depending on adsorbent and adsorbate sizes (Hu et al., 2014).

Increasing concentration of naturally occurring or anthropogenic compounds in the background matrix decreases the adsorption capacity of target compounds because of competitive adsorption onto adsorption sites (Hu et al., 2014).

3 MATERIALS AND METHODS

3.1 Material

Crude glycerol samples were supplied by Milligan Biofuels, Foam Lake, SK, Canada. ACS grade glycerol (99.5 wt% purity) was purchased from Fisher scientific, Canada. Ceramic tubular membranes (diameter 4.7cm, area 443 cm^2, molecular weight cut-off 5 kDa) composed of ZrO_2-TiO_2 with TiO_2 support. The membranes and tubular membrane holder were purchased from Tami Industries, France. Spiral wound polymeric (polyamide) nanofiltration membranes of size 200Da/~1nm (inner diameter: 2.11 cm, length 96.5 cm, area: 639.7 cm^2) were bought from Koch Membrane Systems located in Wilmington, MS, USA. All other chemicals used were analytical grade unless otherwise stated.

3.2 Glycerol purification process

The overall process for glycerol purification is summarized in Figure 3-1 and the steps consist of saponification, acidification, overnight phase separation, solvent extraction and neutralization, followed by membrane filtration under varying temperature, pressure, and flow rate conditions. Activated charcoal treatment and solvent and water evaporation are the final finishing steps.

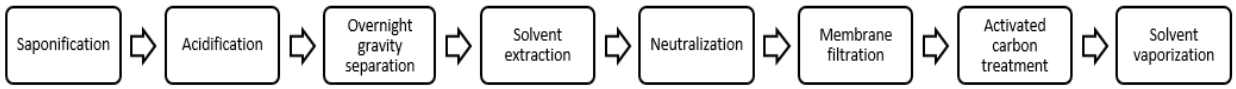

Figure 3-1 Steps in crude glycerol purification process

3.2.1 First step: physico-chemical treatment

Physico-chemical treatment includes a sequential process of saponification, acidification, phase separation and extraction as also described previously. The slightly modified process is as follows: Crude glycerol (glycerol content 40% wt) was mixed with methanol to obtain working glycerol concentration of 20 wt% to reduce glycerol viscosity and improve the flow behavior (viscosity is

~1.2cP) (Dhabhai et al., 2016). It was then heated to 60°C followed by saponification to pH 12.0 using 12.5 M KOH with constant stirring for 30 minutes to convert free fatty acid (FFA) to soap (saponified fatty acids). Acidification was then done with 1M concentrated HCl (98%) to pH 1.0 and stirred for 30 minutes at room temperature (25°C) before overnight separation via gravity sedimentation in separatory funnels. Acidified glycerol separates into two distinct layers: top layer of FFA and glycerol-rich bottom layer and a tiny layer of organic salts at the bottom of the glycerol phase. The upper layer was slowly decanted off and the bottom inorganic salt layer run off to leave the middle glycerol-rich layer to be extracted with volumes of petroleum ether and toluene solvents. The separated glycerol was extracted through solvent extraction using equal volume each of petroleum ether and toluene and then with half volume each of petroleum ether and toluene in a second round to remove residual FFAs. The resultant glycerol was neutralized to pH 7.0 with 12.5 M KOH to obtain the treated glycerol, an enriched form of glycerol, which was used in the membrane filtration experiments.

3.2.2 Second step: membrane filtration in semi-continuous mode

Treated glycerol was further enriched through membrane filtration using a 5 kDa ultrafiltration tubular ceramic membrane at varying temperature, flow rate, and pressure to obtain the final enriched glycerol. It was also enriched using a spiral wound polyamide nanofiltration membrane operated at varying flow rates. A simulated glycerol mixture was also enriched by nanofiltration using the same nanofiltration membranes as a way to simulate rejection of divalent salts by a nanofiltration membrane.

Ultrafiltration for treated glycerol purification

The three parameters that were studied are pressure, flow rate and temperature with the intention to optimize glycerol purity during membrane ultrafiltration of treated glycerol. The parameters were varied over the following ranges: gauge pressure from 345 to 1380 kPa, flow rate

from 50 to 200 mL/min and temperature from 25 to 60°C. The response that was being optimized was glycerol purity, measured in terms of weight percent (wt%).

The experimental runs were determined based on a central composite design (CCD) of experiments done on DesignExpert 9.0 as discussed in a latter section. The schematic for the membrane filtration setup is shown in Figure 3-2 (a) and the actual semi-continuous ultrafiltration apparatus is shown in Figure 3-2 (b).

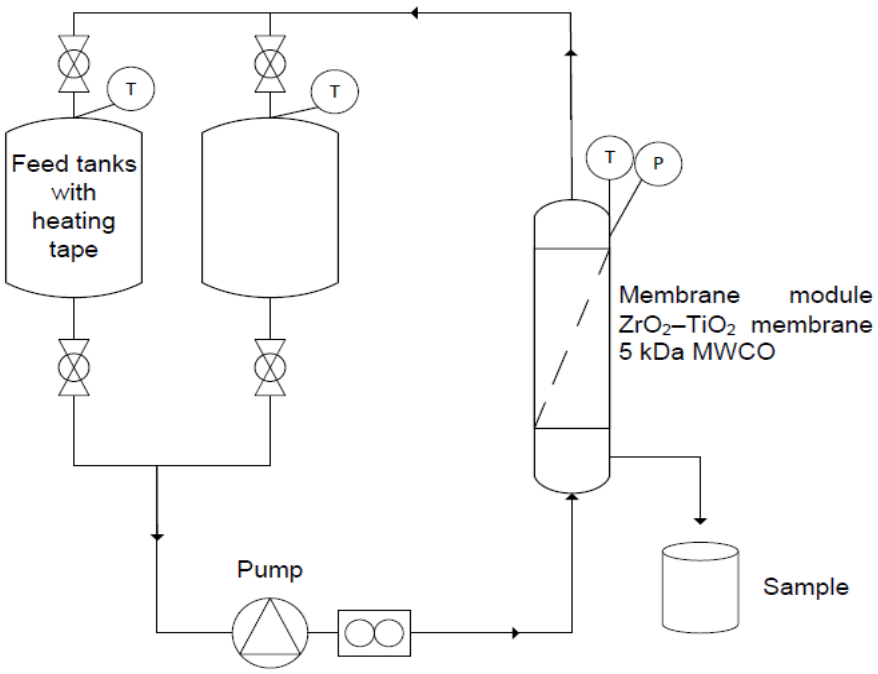

(a) Schematic of the membrane filtration apparatus for glycerol purification

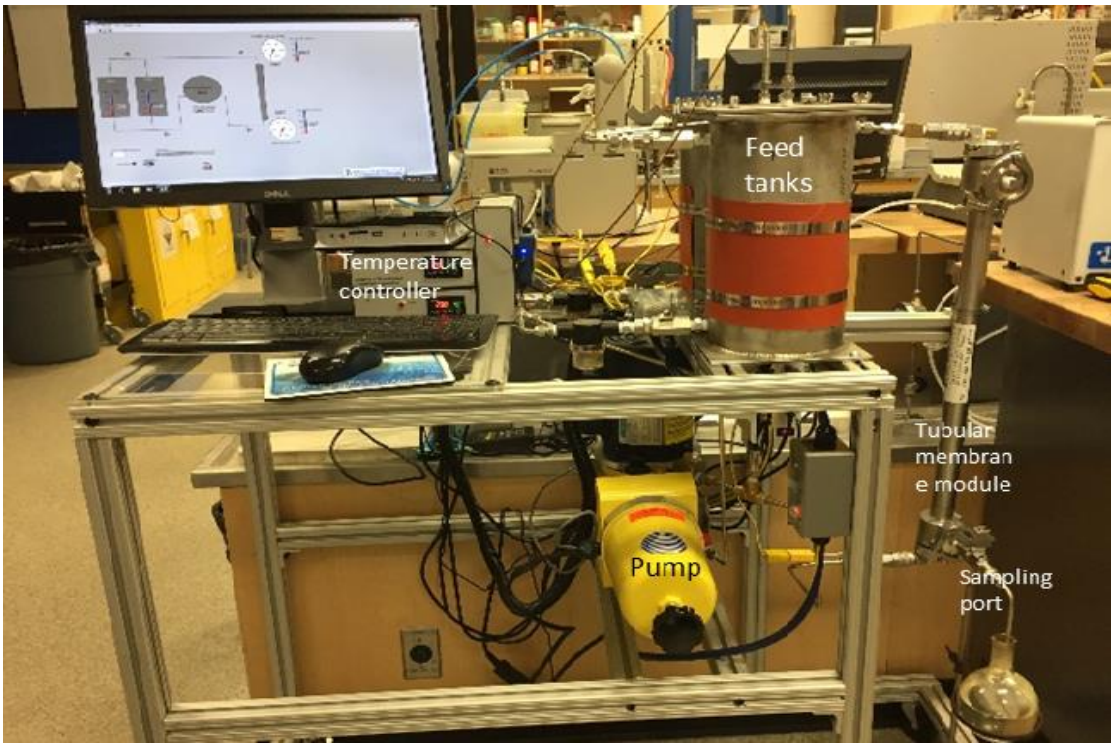

(b) Semi-continuous membrane filtration apparatus

Figure 3-2 Membrane filtration apparatus schematic and real setup

The apparatus consisted of two feed tanks connected with the membrane module (cross flow filtration) through a feed pump. Flow of treated feed in the stainless-steel tubing was controlled by ball valves. Temperature control was achieved using a type K thermocouple (Omega) placed between the tubing and heating tape wrapped around the tubing. Temperature and pressure inside the feed tank and membrane module were monitored constantly and controlled by thermocouples (K type, Omega) and pressure transducers (Honeywell) connected to temperature and pressure monitors which were connected to PC using interface LabVIEW software via USB. The flow pattern in feed tanks was such that the purified liquid can either go to the same tank or different tank after membrane filtration as both the tanks were independently connected to the pump. To study membrane filtration of treated feed, transmembrane temperature, pressure, and

feed flow rate were varied as explained above. The details of membrane filtration experimental design are discussed in the next section.

Treated glycerol from the physico-chemical step (section 3.2.1) was filled in the feed tank up to over the half-way mark. Then the tank(s) were heated and membrane module was heated and pressurized to the desired temperature and pressure before the valves were opened to allow feed flow to the membrane module for filtration. About 15 mL filtrate was collected at each sets of conditions with the process lasting about an hour. After the process, membrane was thoroughly flushed with methanol to clean the foulants and to prepare it for the next round of experiments.

Nanofiltration for purification of simulated glycerol mixture

Purification of a simulated glycerol mixture was performed to study the rejection of divalent salts by nanofiltration membranes. A glycerol mixture consisting of glycerol, a divalent salt ($MgSO_4$ or $ZnSO_4.7H_2O$), water and methanol solvent was made by mixing various volumes of the four chemicals to obtain mixtures or solutions of desired salt content by weight percent. The mixture component of glycerol was kept more or less the same in the range 40 to 45 wt% in all the simulated mixtures or solutions made. As was the amount of water, which ranged from 7 to 12 percent by weight. The amounts of salt and methanol were varied to achieve the desired salt content by weight in the simulated mixtures which ranges from 3-6 wt% for salts. The overall mixture volume was kept more less the same with methanol solvent as the make-weight for countering changes in salt content to ensure a constant final solution volume. Nanofiltration was done by running the simulated glycerol mixture through the membrane setup shown in Figure 3-2 (b) with a spiral wound nanofiltration membrane installed as the tubular membrane module. During filtration, the flow rate was varied from 100 to 200 mL/min while the pre-prepared simulated mixtures run through the membrane already had varying salt contents that had been pre-

determined. As was the case with ultrafiltration samples, nanofiltration samples of 15mL by volume were collected following filtration and water and methanol were vaporized in a rotary evaporator to obtain a final sample of 3-4 mL volume, which was analyzed then analyzed.

Nanofiltration for treated glycerol purification

Treated glycerol purification was also studied using a nanofiltration membrane to observe how such a membrane could improve its purity by rejecting some of the monovalent salt (KCl) content and residual organic molecules. Only flow rate was varied in this phase with the intention to optimize glycerol purity. Temperature was not varied as it could make the membrane more permeable when it is already ideal as a very tight and selective type of membrane. Pressure was also not varied but used as a driving force for the process to establish steady state flow. Pressure values used ranged from 5 – 20 psig (35 – 138 kPa gauge) depending on the feed volume in the piping system and salt content of the feed among other factors. The response that was being optimized was glycerol purity, measured in weight percent (wt%). The experimental runs were determined based on a central composite design (CCD) of experiments done on DesignExpert 9.0 as discussed in a latter section – the same CCD that was used for nanofiltration of simulated glycerol. Mostly only select flow rate values were obtained from this experimental design and used in nanofiltration of treated glycerol since salt content could not be varied in this case as it is pre-determined by the physico-chemical steps.

The schematic for the membrane filtration setup is shown in Figure 3-2 (a) and the actual semi-continuous ultrafiltration apparatus is shown in Figure 3-2 (b) with a spiral wound nanofiltration membrane as the tubular membrane module. As was the case with ultrafiltration samples, nanofiltration samples of 15mL by volume were collected following filtration and water

and methanol vaporized in a rotary evaporator to obtain a final sample of 3-4 mL volume, which was analyzed.

Experimental design and optimization

While there is a great deal of techniques and software for designing and optimizing an experimental process, in this work, the experimental designs were done using DesignExpert version 9.0 (StatEase Inc., USA). Two different experimental designs were done, one for ultrafiltration of treated glycerol (obtained from physico-chemical treatment of crude glycerol) and another for nanofiltration of simulated glycerol mixture and of treated glycerol. In the case of treated glycerol, optimization of the effects of the three process parameters of pressure, flow rate and temperature on glycerol purity obtained from ultrafiltration of treated glycerol was achieved by Central Composite Design (CCD) via Response Surface Methodology (RSM) using the DesignExpert 9.0 software.

As mentioned earlier, the parameter ranges in the design were 345 – 1380 kPa gauge pressure, 50 – 200 mL/min for flow rate and 25 to 60^{o}C for temperature. Pressure limits were chosen based on membrane operability and specification with the lower pressure limit being the minimum pressure required to obtain reasonable filtrate flux or yield and the upper being the most pressure the membrane module can withstand without failing. Flow rate limits were chosen on the basis of what will result in just enough filtrate flux for the lower limit and a controllable flux for the upper limit. The choice of temperature was from room temperature to just before when the solvent (methanol) boils. (Methanol boils at 64.7^{o}C). The response that was being optimized is glycerol purity (in wt%). In the CCD design for ultrafiltration, six replicate center points were chosen and a randomized design used for a more accurate estimation of error due to natural variations and also for a wide sampling range where the standard prediction error could remain a

near constant. Table 3-1 shows the design of experiment for ultrafiltration. The table has been adjusted to points that are measurable on the instrument while eliminating points that cannot be measured due to instrument limitations such as negative pressure points. Instrument limitations could contribute to slight inaccuracies in the Response Surface Methodology's (RSM's) ability to correctly model, predict and optimize the effects of the three parameters on glycerol purity.

Table 3-1 Central composite design (CCD) of experiment for ultrafiltration of treated glycerol

Experimental run	**Temp (°C)**	**Pressure (kPa)**	**Flow Rate (mL/min)**	**Response (glycerol purity wt%)**
1	40	862	125	87.3
2	25	1,380	50	88.2
3	40	862	125	88
4	25	345	50	83.8
5	50	345	200	89.9
6	50	345	50	85.8
7	40	862	125	89
8	40	862	125	88.1
9	50	1,380	200	79.4
10	50	1,380	50	91
11	40	862	125	88.1
12	25	1,380	200	83.4
13	25	345	200	82.3
14	40	862	125	88.1

As for membrane filtration of simulated glycerol mixture, the effects of the two parameters of flow rate (mL/min) and salt content (wt%) on nanofiltration of simulated glycerol mixtures or solutions were optimized using a CCD via RSM on DesignExpert 9.0 software as was the case above for ultrafiltration. The parameter ranges in the design were 100 - 200 mL/min for flow rate and 3-6 wt% for salt content. Flow rate limits were chosen on the basis of obtaining just enough filtrate flux for the lower limit and a controllable flux for the upper limit. The choice of salt content ranges in the simulated glycerol mixture was done based on experience with treated glycerol from

ultrafiltration and from best literature results and also based on what the nanofiltration can handle without having all its pores blocked. With cleaning, not all the salt trapped in the pores of the nanofiltration membrane can be totally removed and the membrane will still be used for purification of treated glycerol at a later stage.

Exercising caution with a reasonable choice of ranges of salt content was therefore deemed necessary. The response that was being optimized is glycerol purity (in wt%). In the CCD design, five replicate center points were chosen and the design randomized for accurate error estimates from natural variation and also for a wider sampling range where the standard prediction error can remain reasonably constant. Membrane filtration of a simulated glycerol mixture was carried out to study optimized nanofiltration of a solution containing divalent salts in preparation for nanofiltration of treated glycerol from physico-treatment of crude glycerol. The experimental design for nanofiltration of simulated glycerol mixtures is as shown in Table 3-2. As for nanofiltration of treated glycerol, selected flow rate values were taken from the CCD for simulated glycerol and used to optimize its purity. Salt content could not be varied during nanofiltration of treated glycerol as it was pre-determined from the physico-chemical stage, especially the amounts of KOH and inorganic acid (HCl) used during saponification, acidification and neutralization along with salt content in crude glycerol from the supplier.

According to literature, the CCD or experimental design approach to experimentation can help determine parameter interactions and the effects of their interactions as well as give a reasonable error estimation (Atadashi et al., 2015). It also cuts the cost and shortens the time of experimentation since the total number of trials is decreased compared to traditional method of holding two factors constant and varying one factor (Atadashi et al., 2015).

Table 3-2 Central Composite Design (CCD) for nanofiltration of simulated glycerol mixture and treated glycerol

		Factor 1	Factor 2
Std	**Run #**	**Flow Rate (mL/min)**	**Salt Content (wt%)**
5	1	79.3	4.5
9	2	150.0	4.5
8	3	150.0	6.6
4	4	200.0	6.0
11	5	150.0	4.5
1	6	100.0	3.0
7	7	150.0	2.4
12	8	150.0	4.5
13	9	150.0	4.5
2	10	200.0	3.0
3	11	100.0	6.0
10	12	150.0	4.5
6	13	220.7	4.5

3.2.3 Finishing steps: solvent vaporization and activated carbon treatment

The third stage of glycerol purification involved adsorption of enriched glycerol with activated carbon as one of the finishing steps in glycerol purification to remove colour and residual FFA. A ratio 1:10 was used as per previous study (Dhabhai et al., 2016). The final stage was water and solvent (methanol, residual petroleum ether, and toluene) evaporation from treated and enriched glycerol to obtain a final volume of 3-4 mL of glycerol sample. Solvent and water evaporation was done by heating glycerol to temperatures above 100^{o}C with constant stirring.

3.2.4 Cleaning of the membrane module and setup

Membrane cleaning entailed disrupting the membrane filtration process by emptying out all the glycerol samples before starting the cleaning process. The membrane setup in this work required cleaning after every 10 hours of operation as the membrane module usually has fouled and/or caked on its surface that could cause concentration polarization. Cleaning therefore became necessary to continue to be able to obtain comparable and consistent results. Membrane cleaning in this work was done by flushing the setup with methanol and circulating it through the entire

system of the setup before draining the cleaning methanol. This was done a few times until a clear methanol solution was obtained at the end. Methanol was chosen because it dissolves glycerol and most polar organics that are part of the treated glycerol that was being purified by membrane filtration. Distilled water could also be used but it is usually difficult to completely vaporize any water in glycerol because of the strong bond glycerol and water tend to form, thanks to their strong hydrogen bond, especially because glycerol has three –OH groups onto which many water molecules can attach.

3.3 Analytical methods

The concentration of glycerol and methanol (in wt%) were determined by a gas chromatograph (GC Agilent 7890 series) using StabilWax column (dimensions 30m x 250µm x 0.5µm; Restek Corp., USA) at 250^{o}C with an FID detector at 300^{o}C, nitrogen at 159 kPa, and helium as the carrier. FFA, mono-, di-, and triglycerides, and esters concentration in crude, treated, and membrane filtered glycerol were determined by HPLC using tetrahydrofuran as mobile phase at 1 mL/min flow rate using a refractive index detector. Water content was determined using an automated Karl Fisher coulometric titrator (Metler Toledo DL32) using methanol for dilution as the titrator was sensitive to a water content of 5 wt% maximum. Crude, treated, and membrane enriched glycerol were characterized by Fourier-Transform infrared (FTIR) spectrometer (Bruker Vertex 70, MA, USA) with ATR module. Each spectrum was the average of 16 co-addition scans with a total scan time of 15s in the range of 4000-400 cm^{-1} at 4 cm^{-1} resolution.

3.4 Techno-economic feasibility analysis and representative process simulation description

For the techno-economic analysis, glycerol purification process was modeled using Aspen Hysys software and the associated capital and operating costs estimated from the simulated process flow diagram, PFD (Appendix B). The process in this simulation followed closely the experimental process described above. Equipment were sized by the software based on the process material and

energy balances and the operating conditions around the equipment. Because of the polar nature of most components in this process, non-random two liquid (NRTL) model was chosen as the fluid simulation package that could accurately simulate the process. Another equally good option would have been universal quasi-chemical (UNIQUAC) model. NRTL was used together with the UNIFAC LLE (liquid-liquid equilibrium) to estimate the missing coefficients, particularly for hypothetical components that were created and added to the Hysys library (Zhang et al., 2003; Apostolakou et al., 2009).

Among the hypothetical components created were KOH, KCl, potassium oleate (K-Oleate), glycerol carbonate and solid catalyst Amberlyst-15, used in ketalization of glycerol. Other chemicals and equipment had their equivalents used to represent them in the simulation. Oleic acid was used to represent free fatty acid component of the crude glycerol, n-pentane and n-hexane to represent petroleum ether by being combined in equal volumes, diethyl ether was used to represent dibutyltin oxide catalyst for glycerol carboxylation, and paraldehyde represented solketal as they have the same chemical formula and comparable physical and chemical properties. A splitter was used to represent a membrane separator with chemical components in the feed being separated using split ratios from literature for ultrafiltration (Singh et al., 2015). All the reactors used in the simulation were conversion types and they are standing in place of the regular CSTR reactors that would be implemented in an industrial process. Pressure drop was assumed to be zero for all equipment mostly because plenty of this process is taking place at atmospheric pressure. Where heating or cooling was required, jacketed reactors were chosen. Where acids were involved, process equipment and their piping systems were made of stainless steel (ss). The rest of the equipment and piping system were made of regular carbon steel (cs) unless stated otherwise.

The following is the description of the modeled process as shown in the PFD (Appendix B). Equal volumes of crude glycerol and methanol were fed into a mixer (MIX-100) to dissolve crude glycerol in the methanol to ensure lower glycerol viscosity, better flow and easier operability. The crude glycerol solution was then passed through a reactor (R-100) where saponification using KOH was carried out at 60^{o}C. The resultant saponified glycerol was fed to a second reactor (R-101) where it was acidified to pH 1 using 1M HCl before being transferred to a high temperature gravity separator (V-100) for gravity sedimentation. Following separation of glycerol (bottom layer) from free fatty acids and residual soap top layer (stream "light liquids") and vapors (Vent-3), the resultant glycerol was fed to a heat exchanger (E-100) via stream 130 for cooling to room temperature before solvent extraction using petroleum ether solvent (stream "PE_Solvent") in a liquid-liquid extraction vessel (V-101). Extracts from this unit were sent into a flash separator (V-103) where petroleum ether was recovered for reuse while the glycerol raffinate was sent into a neutralization reactor unit (R-102) where it was neutralized to pH 7 using KOH. The resultant glycerol was then fed into a membrane separator (M-100) via a pump (L-100) and a feed control valve (VLV-100). In the membrane, some components were rejected according to literature while glycerol solution with methanol and water filtered through (Singh et al., 2015). Methanol solvent and trace water from neutralization were vaporized from glycerol in a flash separator (V-102) before the glycerol was cooled via a heat exchanger (E-102) and sent into a Tee splitter (TEE-100).

The methanol and water vaporized from glycerol in the flash separator unit (V-102) were further sent to another flash separator (V-105) where the vaporized methanol was cooled down just below its boiling point with most of it recovered (stream "Rec_MeOH") to be reused while some of the methanol was allowed to stay in the vapour phase (27%) and was later cooled via a

heat exchanger (E-101) to be used at a later stage in production of glycerol carbonate as the presence of excess methanol solvent speeds up glycerol carboxylation and increases glycerol carbonate yield. At the Tee splitter (TEE-100), the pure glycerol at this point was split into three streams: one stream for pure glycerol product, another stream (191) for solketal production by carboxylation and a third stream (192) for glycerol carbonate synthesis.

The glycerol carbonate synthesis stream (192) was sent into a mixer (MIX-101) where it was combined with recovered methanol stream (194C), which was later used as excess methanol solvent to speed up glycerol carbonate conversion and increase its yield as per literature (Sonatti et al., 2013). The resultant glycerol-methanol mixture (stream L-102) was then passed through a pump to bring it to the desired reaction pressure (3.5 MPa) before being heated via a heat exchanger (E-103) to the desired reaction temperature (80^{o}C) (Sonatti et al., 2013). It was then fed into the reactor (R-104) where it was met via different streams by a heterogeneous catalyst (dibutyltin oxide) and excess CO_2 that was already at reaction conditions (3.5 MPa and 80^{o}C) to produce glycerol carbonate and a waste vapour stream ("Vent-6") (Sonatti et al., 2013). The reaction time was 4 hours (Sonatti et al., 2013). The stream leading to solketal synthesis (191) was fed to a pump (L-101) where its pressure was increased to reaction pressure (12 MPa) before being led into a conversion reactor (R-103) where it was met by the other reactant acetone (stream "Acet") and heterogeneous catalyst Amberlyst-15 (stream "Cat-2") as specified by existing literature to produce solketal (Garcia et al., 2010). The reaction products were maintained at 70^{o}C as that is the ideal recommended outlet temperature for good solketal yield according to literature on synthesis (Garcia et al., 2010). The reaction time was 1.5 hours. To separate excess acetone and condensation water from solketal product (stream 201), the reaction products were sent to a flash separator (V-103) where acetone with trace water was vaporized before being cooled down via a heat exchanger

(E-104) and recovered. Solketal stream (202) was sent to a Tee-splitter (TEE-101) where it was split equally into a pure solketal product outlet and a recycle stream (204) that was sent back to the reactor to improve conversion since glycerol ketalization conversion is only 35% but rises highly with product recycle, as per literature (Garcia et al., 2010). The recovered acetone can be reused as a reactant since an acetone-glycerol molar ratio of between 6/1 and 10/1 is required in this process for 80-90% conversion (Garcia et al., 2010).

4 RESULTS AND DISCUSSION

This section presents the experimental results and a discussion of these results.

4.1 Effectiveness of the physico-chemical treatment

Saponification with 12.5M KOH of crude glycerol containing free fatty acids resulted in the converting of the free fatty acids to saponified fatty acids according to Equation 4-1 (Ardi et al., 2015).

$$R - COOCH_3 + KOH \rightarrow R - COOK + CH_3OH \quad (4\text{-}1)$$

Acidification of saponified crude glycerol with HCl results in formation of two distinct layers during overnight separation: an FFA-rich top phase and a bottom glycerol-rich phase. Below the glycerol-rich bottom phase was also a small inorganic salt phase, which was run-off slowly using a tap at the bottom of the separatory funnel during this step. Since the FFA-rich layer had a lower density than the glycerol phase, it floated on top with a clear separation and was decanted off slowly (Dhabhai et al., 2016). The H+ ions in the mineral acid HCl converted saponified fatty acids (SFAs) to insoluble free fatty acids (FFAs), which stayed in their top layer (Dhabhai et al., 2016) as shown in Equation 4-2.

$$RCOOK + H^+ \rightarrow R - COOH + K^+ \quad (4\text{-}2)$$

Neutralization with strong KOH followed the overnight separation and solvent extraction of the acidified crude glycerol to produce the water-soluble KCl salt (342g/L at 20^{o}C). Neutralization converted residual FFAs and FAME in glycerol to soaps. Saponified fatty acids (SFAs) contribute to MONG content while any residual soap formed added to the ash and MONG contents of the final enriched glycerol. This phenomenon might limit the achievable degree of glycerol enrichment from the physico-chemical stage (Ardi et al., 2016; Kongjao et al., 2010). Glycerol layer composition and MONG content are highly dependent on the acid used for

acidification and final acid pH (Manosak et al., 2011). A final acidification pH of 1 favours glycerol enrichment and decreased FFA and inorganic salt formation (Kongjao et al., 2010). Glycerol purity in the treated feed following the sequential physico-chemical treatment was 82.5 wt% with water content in the range 4.0-8.0% (Table 4-1) and the rest of the content being FFAs, glycerides, inorganic salts and FAME that were not completely separated from glycerol phase. This is a better enrichment outcome than the 51.4 wt% that Ooi et al achieved after some form of physico-chemical treatment (Xiao et al., 2013).

Table 4-1 Enrichment of glycerol after each stage of physico-chemical treatment

Stage of physic-chemical treatment	**Glycerol* (wt%)**	**Methanol (wt%)**	**Water (wt%)**
Crude glycerol	40.0	30.0	5.0
Saponification-acidification and Overnight separation	75.4	0	2.5-4.0
Petroleum ether extraction	82.5	0	2.5-4.0
Toluene extraction	86.4	0	2.5-4.0
Neutralization**	83.5	0	4.0-8.0

*Average of glycerol percentage for >40 batches of treated glycerol after solvent evaporation.

**Neutralization slightly reduces the glycerol purity as water is generated in acid-base neutralization reaction.

Table 4-1 shows the enrichment in glycerol purity after each stage of physico-chemical treatment which is the average of over 40 batches (± 2.97). The first combined steps of saponification, acidification, and phase separation enhanced glycerol purity to 82.5 wt% from the initial 40 wt% purity, which is more than double enhancement in glycerol purity. For solvent extraction, two different solvents – petroleum ether and toluene - were employed as the solvent type and ratio affect glycerol yield (Hunsom et al., 2013). Both solvents were employed sequentially for two rounds of extraction with each and both were equally effective in enhancing

glycerol purity by removing FFA from the crude glycerol and increasing glycerol purity to 86.4 wt%. The last step of the treatment – neutralization - led to slight decrease in glycerol purity due to formation of water and salt in the acid-alkali neutralization reaction (Dhabhai et al., 2016). A maximum of 83.5 wt% glycerol purity was obtained after physico-chemical treatment, a number that is slightly lower than that obtained in other similar studies such as 88.6 wt% by Dhabhai et al., Manosak et al., who reported 95.74 wt%, and Xiao et al. who achieved greater than 94 wt% (Dhabhai et al., 2016; Manosak et al., 2011; Xiao et al., 2013).

Table 4-2 Composition of crude, treated and enriched glycerol

Component	**Crude glycerol (wt%)**	**Treated glycerol* (wt%)**	**Enriched glycerol* (wt%)**
Glycerol	40.00	86.40	93.70
Methanol	24.00	0	0
Water	5.00	3.00	3.00
Triglycerides	0.13	0.03	0.03
Diglycerides	0.68	0.03	0.02
Monoglycerides	1.90	0.25	0.12
Free Fatty Acids (FFAs)	13.20	0	0
Esters	10.00	1.52	0
Ash	4.90	2.80	1.2
Total	99.80	93.93	98.07

* After physico-chemical treatment and solvent evaporation

** Enriched glycerol is glycerol after membrane filtration, activated charcoal adsorption, and solvent and partial water evaporation

In the current work, glycerol yield was an average of more than 40 batches, hence slight variation in yield was obtained (±2.97). Furthermore, Table 4-2 presents the overall composition of crude, treated, and enriched glycerol. Treated glycerol refers to the purified glycerol obtained after the physico-chemical treatment, while enriched glycerol is obtained after membrane filtration

and activated carbon adsorption of treated glycerol. In both cases, solvent and partial water evaporation was carried out before sample analysis. Enrichment in glycerol purity was obtained after physico-chemical treatment and membrane filtration. A near 100% removal of FFA and methanol, and approximately 85% removal of esters were achieved, while there was significant reduction in ash and glycerides (mono-, di- and tri-) content after the physico-chemical treatment. The total composition of crude and treated glycerol is not 100%, the reason can be the presence of minor unidentified colloidal particles formed during the treatment (in case of treated glycerol) or biodiesel production (for crude glycerol).

4.2 Optimized semi-continuous membrane purification of glycerol

In this section, the effects of the purification processes of ultrafiltration and nanofiltration on treated glycerol and the effects of nanofiltration on simulated glycerol mixture are discussed and their respective response surface plots presented along with a discussion of their statistical analyses and analyses of variables (ANOVA) for their deduced models.

4.2.1 Ultrafiltration purification of treated glycerol

The best results for membrane filtered enriched glycerol are presented in Table 4-3. As compared to treated glycerol from the physico-chemical steps, further enrichment in glycerol purity was obtained after membrane filtration with a maximum of 93.7 wt% glycerol purity being obtained, which is just under the technical grade (95 wt%). Membrane treatment was successful in removing colloidal particles, oil droplets, and some other components such as salt deposits, which were not completely removed during the physico-chemical treatment steps.

Membrane performance in enhancing glycerol purity was studied in terms of the effects of parameters – temperature, pressure, and feed flow rate - and the parameter-parameter interactions effects on glycerol purity. Membrane filtration was studied using a 5 kDa UF ceramic tubular membrane. The membrane flux was not studied as the flux was high enough and stayed almost the

same at all the experimental conditions with 95% glycerol recovery following membrane filtration. Also, the effects of varying solution pH was not studied as ceramic membranes have great chemical stability and the final treated glycerol was always kept at neutral pH, which makes it safe even for the polymeric nanofiltration membrane. The underlying assumptions were that impurities with MWCO >5 kDa like oil droplets and colloidal particles would be retained by the membrane while glycerol (92.1 Da) would filter through membrane pores as filtration is based on the MWCO of a material.

Table 4-3 Representative results of the membrane filtration study after physico-chemical treatment

Temperature (ºC)	**Flow Rate (mL/min)**	**Pressure (kPa g)**	**Glycerol Purity (wt %)**
25	50	345	83.8 ±3.38
25	50	690	87.8 ±2.55
25	50	1380	88.2 ± 0.56
40	50	345	92.4 ±1.53
40	50	690	91.0 ± 2.86
40	100	690	92.2 ±5.39
40	125	862	88.1 ± 0.86
50	50	345	85.8 ± 5.72
50	50	690	93.7 ± 4.39
50	50	1380	91.0 ± 4.86
50	100	345	86.6 ± 4.42
50	100	690	87.3 ± 3.63
50	100	1380	86.8 ± 2.88
50	200	690	89.9 ± 6.22
60	50	345	75.8 ± 0.33
60	50	690	75.8 ± 0.19
60	50	1380	77.1 ± 0.53
60	100	690	77.9 ± 1.01
60	125	862	77.1 ± 0.99

From the best results obtained from physico-chemical treatment and membrane filtration at different optimization conditions, (Tables 4-1 to 4-3), it can be observed that the highest glycerol purity results of 93.7 wt% were obtained at 50˚C temperature, 50 mL/min flow rate and 690 kPa pressure. The next best glycerol purity results achieved were 92.4 and 92.2 wt% glycerol purity

obtained at 40^{o}C, 50 mL/min and 345 kPa; and 40^{o}C, 100 mL/min and 690 kPa respectively. These glycerol purities are just under technical grade and are a huge improvement on the 82.5 wt% purity obtained after the initial sequential physico-chemical treatment steps.

Organic molecules and colloids of larger molecular size (MWCO) are rejected by the ultrafiltration membrane of 5 kDa MWCO due to their large molecular size and were thus unable to sieve through membrane pores into the permeate (Wang et al., 2011; Singh et al., 2015; Peters et al., 2010). This resulted in further enhancement in glycerol purity.

Relatively low glycerol purity results were obtained at 25^{o}C compared to 40 and 50^{o}C and this can be attributed to higher glycerol viscosity at room temperature (~1.2cP vs 0.8cP from 40 to 50^{o}C) (Dhabhai et al., 2016). This affects the flow properties of glycerol and the ability to sieve through the membrane and be separated from the impurities (Dow Chemical Company, 2016). Glycerol purification by the combination of physico-chemical treatment and membrane filtration works best at lower glycerol viscosity as this results in more solute coming into contact with membrane surface and increasing the chances of the smaller components being filtered through the pores by sieving, as per the primary filtration mechanism in Darcy's law, which governs ultrafiltration (Singh et al., 2015; Peters et al., 2010). With improved feed flow due to low glycerol dynamic viscosity as a result of elevated temperatures, bigger particles, mostly organics, are also easily rejected by membrane sieves (pores) of low MWCO (5kDa) at temperatures from 40 to 50°C. The result is more glycerol, water and solvent (methanol) sieving through the membrane and more of the colloids and organic macromolecules being excluded (Wang et al., 2011; Singh et al., 2015; Peters et al., 2010). Methanol and water are later vaporized hence increased glycerol purity. This is why the highest glycerol purity results (92.2 - 93.7 wt%) were obtained at the high temperatures of 40 to 50°C.

Pressure is used as the driving force in ultrafiltration and it creates the required force to enhance the sieving through membrane pores of molecules smaller than 5 kDa molecular weight (Wang et al., 2011; Singh et al., 2015; Peters et al., 2010). In this work, increasing pressure increased glycerol purity up to pressure values above 700 kPa. It is to be noted that, not all molecules smaller than the MWCO are able to sieve through as some get blocked by adsorbed particles on membrane surfaces and do not come into contact with the membrane surface (Wang et al., 2011; Singh et al., 2015; Peters et al., 2010). Looking at the results in terms of flow rate, increasing the flow rate generally decreases the purity of the resultant glycerol.

It is to be noted that no consistent results were obtained at 60^{o}C and this is attributable to solvent (methanol) evaporation and buildup of its vapor above the treated glycerol solution. Evaporating methanol meant increasing glycerol viscosity and lack of consistent flow and sieving through the membrane filtration system, resulting in low glycerol purities after optimized membrane filtration (70-80 wt%).

Response surface methodology (RSM) for ultrafiltration of treated glycerol

With regards to the combined effects of the three parameters of temperature, pressure and flow rate and the possible effects of their factor-factor interaction on glycerol purity, response surface plots were constructed from the response (glycerol purity) of every two parameters and the results are as presented in Figure 4-1 (a)-(c).

The interaction between pressure and temperature (Figure 4-1a) seems to give the best results at higher temperatures from 40 towards 50°C and lower pressure (towards 345 kPa) as this is the area of highest resultant glycerol purity. The increase in purity is thus in the direction of red colour from the barely blue edge through the largely green middle area. Looking at the contours at the bottom of the response surface plot in Figure 4-1a in the yellow area and their gradients at a point and over small parts of a line, it can be seen that contour for lower temperature and pressure

(30^{o}C and 759 kPa) were more gently sloping than those at higher temperature and pressure (35^{o}C and 1173 kPa), which are steeper at starting points. This can be interpreted to mean a higher rate of increase in response (purity) at higher temperature and higher pressure than at lower temperature and lower pressure. The contour for higher temperature and higher pressure is especially steeper at higher pressure areas even when the temperature is not particularly as high as 35^{o}C. This can be interpreted to mean higher effect of pressure up to 1173 kPa on purity at even temperatures under 35^{o}C.

Temperature and flow rate response surface plots (Figure 4-1b) give the best results at high temperature (up to 50^{o}C) and low flow rate (100 - 50 mL/min). Looking at the contours at the bottom of the response surface plot, which are initially parallel and running diagonally from right to the left, it can be seen that glycerol purity is increasing diagonally towards the left side area of low flow rate (<80 mL/min) and higher temperature (over 45 to 50^{o}C). It can therefore be interpreted to mean glycerol purity is increasing with increasing temperature and decreasing flow rate. The diagonal lines are no longer parallel towards the left end when they become steeper, meaning higher rate of increase in purity with decreasing flow rate (80 to 50 mL/min) and increasing temperature (45 to 50^{o}C).

The combined effect of pressure and flow rate (Figure 4-1c) has its best glycerol purity results to the left side in the region of high pressure (1173 to 1380 kPa) and low flow rate (50mL/min). Glycerol purity is increasing from the green region to the red region. With regards to contours at the bottom of the pressure and flow rate response surface plot, especially the inner-most contour, it can be seen that the contour is steeper at the starting point on the right side in region of high flow rate (200 to 140 mL/min) and low pressure (345 to 552 kPa) before it becomes more gentle at a latter stage. This can be interpreted to mean that the rate of increase in glycerol

purity at high but decreasing flow rate (200 to 140 mL/min) and low pressure (345 to 552 kPa) is initially very high before the rate of increase in purity steadies at a slower rate as can be seen from the contour becoming a near straight line.

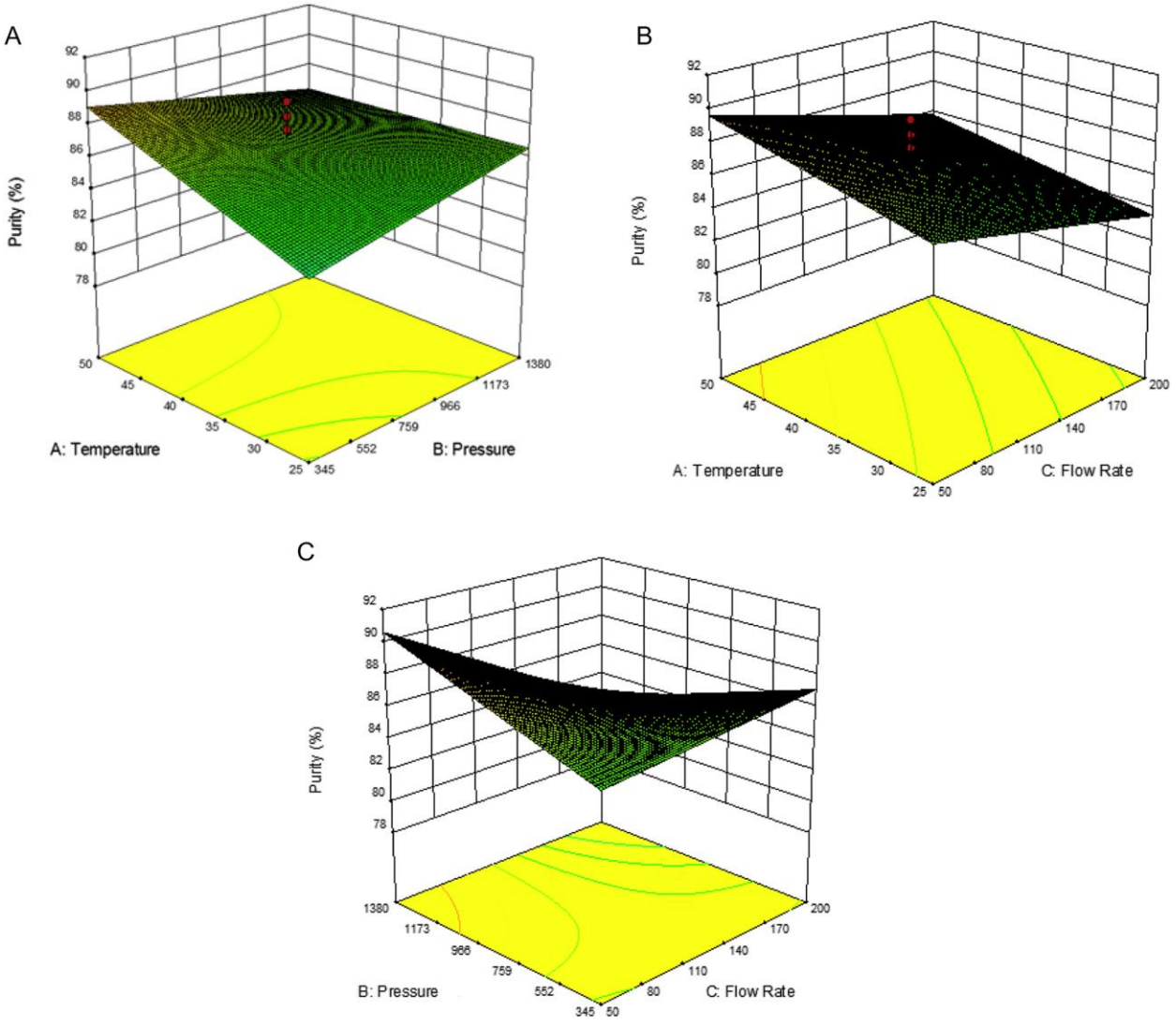

Figure 4-1 Response surface plots showing the effects of parameters on glycerol purity: (a) effects of temperature (°C) and pressure (kPa) on glycerol purity at a flow rate of 125 mL/min; (b) effects of temperature (°C) and flow rate (ml/min) on glycerol purity at a pressure of 862.5 kPa; and (c) effects of flow rate (ml/min) and pressure (kPa) on glycerol purity at a temperature of 40°C

Overall in terms of the effects of the interactions of the three parameters on glycerol purity, the best glycerol purity results were obtained at high values for temperature (40-50˚C), low flow rate (50-100 mL/min), and pressure in the higher range (690-1380 kPa).

Statistical analysis for ultrafiltration of treated glycerol

To describe the effects of these three parameters (temperature, pressure, and feed flow rate) on glycerol purity, a two-factor interaction (2FI) model was found to be the most appropriate to describe the relationship. On the basis of sequential model sum of squares (Type I) from statistical analysis, a two-factor interaction (2FI) vs mean model was found to be most appropriate because its additional terms were significant, and the model was not aliased. A 2FI was also found to be the most appropriate by the Lack of Fit Tests method as it had insignificant lack of fit (Prob >f = 0.0002). On the basis of the model summary statistics, 2FI model was also found to be the most appropriate to describe this optimization process as it maximized Adjusted R-Squared and predicted R-Squared.

Analysis of variable (ANOVA) for 2FI model for ultrafiltration of treated glycerol

Tables 4-4 present the analysis of variable (ANOVA) and standard error results for ultrafiltration of treated glycerol.

Table 4-4 ANOVA for partial sum of squares – Type III

Source	**Sum of Squares**	**df**	**Source**	**F Value**	**P Value (Prob > F)**
Model	96.48	6	16.08	2.79	0.1028
A - Temp	12.79	1	12.79	2.22	0.1800
B - Pressure	0.005	1	0.005	0.000868	0.9773
C - Flow Rate	23.81	1	23.81	4.13	0.0816
AB	14.58	1	14.58	2.53	0.1557
AC	0.18	1	0.18	0.031	0.8647
BC	45.12	1	45.12	7.83	0.0266
Residual	40.34	7	5.76		
Lack of Fit	38.88	2	19.44	66.57	0.0002
Pure Error	1.46	5	0.29		
Corr Relation	136.8213				

A value of Prob>F less than 0.05 indicates that the model terms are significant. BC is thus a significant model term in this case. “Adeq Precision” measures signal to noise ratio with a ratio greater than 4 being desirable. The current ANOVA gives “Adeq Precision” of 5.007 indicating an adequate signal. This model can thus be used to navigate the design space.

Table 4-5 Coefficient estimate, standard error and confidence interval

Factor	**Coefficient Estimate**	**df**	**Standard Error**	**95% CI Low**	**95% CI High**	**VIF**
Intercept	86.49	1	0.65	84.97	88.02	
A-Temperature	1.25	1	0.84	-0.74	3.24	1.00
B-Pressure	0.025	1	0.85	-1.98	2.03	1.00
C-Flow Rate	-1.73	1	0.85	-3.73	0.28	1.00
AB	-1.35	1	0.85	-3.36	0.66	1.00
AC	-0.15	1	0.85	-2.16	1.86	1.00
BC	-2.37	1	0.85	-4.38	-0.37	1.00

Based on the table of coefficients, standard error and 95% confidence intervals, the final equation in terms of coded factors is:

$$\text{Purity} = 86.49 + 1.25*A + 0.025*B - 1.73*C - 1.35*AB - 0.15*AC - 2.37*BC \quad (4\text{-}3)$$

Equation 4-3 in terms of coded factors can be used to make predictions about the response for given levels of each factor. By default, the higher levels of the factors are coded as +1 and the low levels of the factors are coded as -1. The coded equation is useful for identifying the relativity impact of the factors by comparing the factor coefficients.

Equation 4-4 gives the final equation that describes the response (purity) in terms of the three actual parameters of temperature, pressure and flow rate that are being optimized.

Purity (%) = 71.5% + 0.300*T (^{o}C) + 0.016*P (kPa) + 0.036*FR (mL/min) – 0.000209*T*P – 0.00016*T*FR – 0.0000612*P*FR (4-4)

T being temperature, P is pressure and FR is flow rate.

This equation can be used to make predictions about the response (% purity) in terms of given levels of each factor. The levels should be specified in the original units for each factor. This equation can however not be used to determine the relative impact of each factor as the coefficients are scaled to accommodate the units for each factor and the intercept is not at the center of the design space.

4.2.2 Purification of simulated glycerol mixture by nanofiltration

From initial test results (Table 4-6) using the divalent salts of magnesium sulfate and zinc sulfate heptahydrate with salt contents of 5.0 wt% and 4.0 w% respectively, it is clear that nanofiltration improves the purity of simulated glycerol mixtures from initial 88.8 and 86.9 wt% to 98.8 and 96.6 - 100.0 wt% for magnesium sulfate and zinc sulfate heptahydrate respectively. This is consistent with theory, which argues that nanofiltration membranes reject 100% of divalent salts (Peter et al., 2010). In case where a purity of 100 wt% was not attained, the remaining 1.2-3.4 wt% was mostly water. All the initial methanol content was evaporated and no methanol content was detected in any samples. While water content in the final glycerol following nanofiltration tends to vary, it depends on the effectiveness of the vaporization method for water and methanol. Evaporation in a rotary vaporizer has been proven before in this work to be most effective though an average of 1.0 wt% water is always left in purified glycerol, depending on the initial and final amounts of water and glycerol involved and the effectiveness of their affinities to each other in terms of intermolecular hydrogen bonding (Pagliaro et al., 2008).

Glycerol and water have strong affinity for each other due to the hydroxyl groups present in each of them that form strong intramolecular and intermolecular hydrogen bonds between them. However, since equal volumes of glycerol and water were used in these simulated glycerol mixtures to begin with, apart from the effectiveness of the water-solvent evaporation method, only the ability of each of the rejected divalent salts to retain some water in itself might further account for additional differences observed in the enriched filtered glycerol samples and higher solvent flux over solutes in the glycerol that filtered through the membrane according to solution-diffusion model of nanofiltration (Ramaswamy et al., 2013).

Table 4-6 Simulated glycerol purity results for initial test samples of divalent salts

Sample Name	**Purity (wt%)**
Unfiltered $MgSO_4$	88.8
Filtered $MgSO_4$	98.8
Unfiltered $ZnSO_4.7H_2O$	86.9
Cycle-1 $ZnSO_4.7H_2O$	100.0

From the nanofiltration results (Table 4-7) obtained from simulated crude glycerol based on the experimental design in Table 3-2 using varying zinc sulfate heptahydrate salt contents (no magnesium sulfate used) and flow rate, it can be observed that up to 100 wt% glycerol purity can be obtained from salts of initial purities of 86 – 88 wt%. While a purity of 100 wt% glycerol was attained sometimes from a simulated glycerol mixture with initial salt contents of 4.5 wt% to 6 wt% or more at various flow rates, it was more likely to be obtained from a simulated mixture with lower initial salt contents (2.0 to 3.0 wt%). Even though the rejection of the divalent salts is 100%,

some of the water is retained by the rejected salts and how that affects the amount of water left in the filtered glycerol has some effect on how much water can be retained by the final filtered glycerol, hence the slight variations in final purities observed. Starting with an initial salt content of 4.5 wt% in the simulated glycerol, the highest purities obtained are 98.6 to 98.8 wt% at 150 mL/min and 79.3 mL/min respectively, meaning around that range of flow rate the highest glycerol purities are obtained from nanofiltration of a simulated glycerol solution. For simulated glycerol mixtures of low salt content (2.4 to 3.0 wt%), a final purity of 100 wt% for filtered glycerol samples was obtained from all flow rate ranges from 100 to 200 mL/min. A final purity of 100 wt% glycerol was obtained at 100 mL/min when the initial simulated glycerol mixture contained 6 wt% salt.

Table 4-7 Purity results for nanofiltration of simulated glycerol samples

Run #	**Factor 1**	**Factor 2**	**Response**	
	Flow Rate (mL/min)	**Salt Content (wt%)**	**Glycerol Purity (wt%)**	**Product Water Content**
1	79.3	4.5	98.8 ± 1.0	0.6
2	150.0	4.5	96.0 ± 3.0	1.0 - 2.0
3	150.0	6.6	96.6	1.4
4	200.0	6.0	91.6 ± 8.0	3.1 - 3.9
5	150.0	4.5	96.0 ± 3.0	1.0 - 2.0
6	100.0	3.0	100.0	0
7	150.0	2.4	100.0	0
8	150.0	4.5	96.0 ± 3.0	1.0 - 2.0
9	150.0	4.5	96.0 ± 3.0	1.0 - 2.0
10	200.0	3.0	100.0 ± 0.0	0
11	100.0	6.0	100.0 ± 0.0	0
12	150.0	4.5	96.0 ± 3.0	1.0 - 2.0
13	220.7	4.5	93.9 ± 5.6	2.0 - 2.2

Fractionation in nanofiltration depends on charge with more charged ions better retained than monovalent ions as discussed in depth in Literature Review (Manttari et al., 2013). This explains why the divalent salts (both $MgS0_4$ and $ZnSO_4.7H_2O$ in Table 4-6 and $ZnSO_4.7H_2O$ in Table 4-7) are retained inside the membrane and sieved out from the final glycerol as these divalent salts have more charge (+2) than a monovalent salt like KCl would have. Filtration parameters greatly affect nanofiltration membrane's ability to retain (Manttari et al., 2013). Because of solution-diffusion mechanism of tight nanofiltration membranes, retention tends to decrease with constant flux when the concentrate of solutes increases (Manttari et al., 2013). This explains why lower purities were obtained at higher salt contents (6 wt% or higher) at constant flow rate and pressure hence constant flux as the lower solute contents (3 wt% or less) since the former represents higher concentrate. This is attributable to solute diffusion increasing with increasing concentration (Manttari et al., 2013). Increasing pressure tends to increase solvent flux but the solute flux depends on its concentration inside the membrane solution as per the solution-diffusion model and the result is increased retention (Manttari et al., 2013). In cases where the solute concentrations are high like the case of 6 wt% and over, the resultant purities for glycerol are lower meaning solute fluxes are higher in the purified glycerol.

Response Surface Methodology for nanofiltration of simulated glycerol mixture

With regards to the combined effects of the two parameters of salt content and flow rate and the probably combined effects of their interaction with each other on glycerol purity, a response surface was constructed from the response results (Table 4-7) as presented in Figure 4-2. The interaction between salt content and flow rate from the response surface plot gives the best results in the region of lower salt content (towards 3 wt% or less) and lower flow rate (towards 100 mL/min) or sometimes towards the region of lower flow rate (~100 mL/min) and high salt

content, though these values have been flagged as higher than predicted based on the design equation (Equation 4-6).

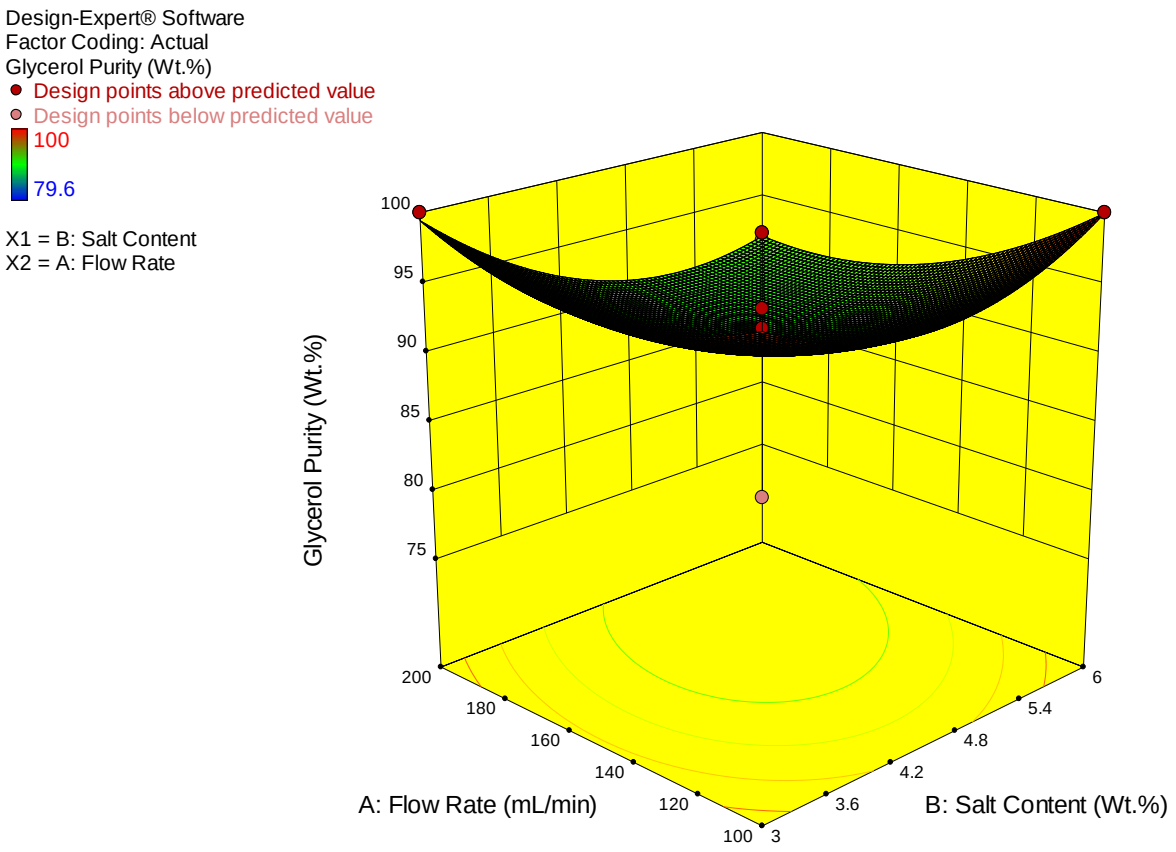

Figure 4-2 Response surface for simulated glycerol mixture samples

The contours at the bottom of the response surface plot also show the same trend with increasing purity results towards the near diagonal corner of lower flow rate (~100 mL/min) and lower salt concentration (~3 wt% salt content). In terms of the contour gradients at a point, the contour gradients are higher on the sides of the contour lines in the region of higher salt content and flow rate and then the gradients decrease with decreasing salt content and flow rate. This means that the rate of increase in purity is accelerated initially in the region of high salt content

and high flow rate as the values of both are decreased and then the purity increases slowly as it approaches 100% glycerol purity. The contours are linear closest to 100% glycerol purity meaning the rate of increase in purity is linear with changes in salt content (wt%) and flow rate at this point.

Statistical analysis for simulated glycerol mixture

Using Sequential Model Sum of Squares (Type I), the suggested model for this set of results is Quadratic vs 2FI because it is the highest order polynomial where the additional terms are significant and the model is not aliased. By Lack of Fit Tests, a Quadratic model is the suggested model because it has insignificant lack-of-fit. Using the Model Summary Statistics, the Quadratic model is the suggested model since this is the model maximizing the "Adjusted R-Squared" and the "Predicted R-Squared". In summary, the Quadratic model is the suggested model since cubic model and higher ones are aliased.

Analysis of variance (ANOVA) for the quadratic model

Table 4-8 Coefficient estimate, standard error and confidence interval

Factor	**Coefficient Estimate**	**df**	**Standard Error**	**95% CI Low**	**9%CI High**	**VIF**
Intercept	90.84	1	2.37	85.24	96.44	
A – Flow Rate	-1.92	1	1.87	-6.34	2.51	1.00
B – Salt Content	-1.65	1	1.87	-6.08	2.78	1.00
AB	-2.10	1	2.65	-8.36	4.16	1.00
A^2	2.90	1	2.01	-1.85	7.65	1.02
B^2	3.87	1	2.01	-0.87	8.62	1.02

Final equation in terms of coded factors:

$$\text{Glycerol Purity} = 90.84 - 1.92*A - 1.65*B - 2.10*AB + 2.90*A^2 + 3.87*B^2 \quad (4\text{-}5)$$

Final equation in terms of actual factors:

$$\text{Glycerol purity} = 143.59 - 0.26*\text{Flow Rate} - 12.39*\text{Salt Content} - 0.028*\text{Flow Rate}*\text{Salt Content} + 0.00116*(\text{Flow Rate})^2 + 1.72*(\text{Salt Content})^2 \quad (4\text{-}6)$$

The equation in terms of actual factors can be used to make predictions about the response for given levels of each factor. Here, the levels should be specified in the original units for each factor. This equation 4-6 should not be used to determine the relative impact of each factor because the coefficients are scaled to accommodate the units of each factor and the intercept is not at the center of the design.

4.2.3 Effects of nanofiltration on treated glycerol

Nanofiltration of treated glycerol using the 200 Da sized spiral wound polyamide nanofiltration membrane at selected flow rates from the CCD design for nanofiltration gave the results shown Table 4-9.

Table 4-9 Glycerol purity results for nanofiltration of glycerol at various flow rates

Sample	Flow rate (mL/min)	Average purity (wt%)	Product water content (wt%)
A	80	97.2 ± 1.0	1.0
B	125	94.9 ± 1.0	1.8
C	150	91.3 ± 1.5	4.0
D	200	91.4 ± 1.9	4.2
E	221	89.5 ± 0.9	5.0

From the results, it can be observed that the highest purities obtained from nanofiltration of treated glycerol are 97.2 and 94.9 wt% at 80 and 125 mL/min flow rates, both of which can be considered technical grade. The impurities left in glycerol following this enrichment are water and salt (KCl), each of which varies from 1-3 wt%. Nanofiltration works through possibilities of separation transport by diffusion and convection for a successful separation (Manttari et al., 2013). Nanofiltration membranes retain over 90% of the uncharged molecules above the molecular

weight cut-off and therefore specific small molecules can be fractionated into permeate from a solution containing different molecules (Manttari et al., 2013). This means glycerol, water and methanol among other small uncharged molecules sieved through the membrane pores while bigger residual organic molecules not removed in the physico-chemical stage were retained inside the membrane as part of the concentrate. Other factors like polar interactions and hydrophobic interactions determine achievable retention during membrane filtration; a high dipole moment enhances transmission through membrane – the molecule (dipole) tends to turn itself against the membrane and can easily pass through the membrane especially when the membrane pore size is bigger than that of the molecule (Manttari et al., 2013; Van der Bruggen et al., 2001). For molecules of the same size as the membrane pore, retention of polar molecules is typically smaller (Manttari et al., 2013).

Fractionation also depends on charge with more charged ions better retained than monovalent ions (Manttari et al., 2013). Filtration parameters have a remarkable effect on nanofiltration membrane's ability to retain (Manttari et al., 2013). Due to solution-diffusion mechanism of tight nanofiltration membranes, retention tends to decrease with constant flux conditions when the concentrate of solutes increases or when the solvent temperature increases (Manttari et al., 2013). High temperatures and pH could also change the membrane structure of polymeric membranes and decrease retention (Ramaswamy et al., 2013). This is why temperature and solute concentration of solution were not varied for treated glycerol since the goal is to ensure more retention of impurities and only permeation of glycerol and the tiny solvent particles. Increasing pressure tends to increase solvent flux but the solute flux depends on its concentration in the membrane, as per the solution-diffusion model and the result is increased retention (Manttari et al., 2013).

Organic molecules are sieved from feed due to their larger sizes than pores or because of other interaction mechanisms with the membrane surface such as polarity or charge, when such exists otherwise retention generally increases with increasing molecular weight above pore size or membrane molecular weight cut-off (Manttari et al., 2013). While there are many models to describe transport and retention of inorganics, the basis for simulation of ions retention is the extended Nernst-Planck equation (Manttari et al., 2013).

4.3 Crude, treated and enriched glycerol characterization by Fourier-Transform Infrared (FTIR)

Samples of enriched glycerol (treated and membrane purified) were characterized by FTIR and their spectra compared with spectra of crude glycerol and pure ACS grade glycerol. Glycerol from physico-chemical treatment was considered the treated glycerol while that from the subsequent membrane filtration stage was classed as the purified glycerol, but both are definitely enriched forms of glycerol and are very close in terms of purities. A spectra of the characterization is as shown in Figure 4-3.

The final spectra were normalized as follows. A background scan was run first on the instrument with no sample in it (a blank sample). A sample scan was then run for all the four samples under exactly the same conditions as the blank scan in terms of method and settings used. A background correction was then performed by subtracting the background scan results from the sample results to get the real FTIR spectra. A normalization was then done by dividing FTIR absorbance values for all the spectra by the highest absorbance value to reset the y-axis to values from 0 to 1 as can be seen in Figure 4-3.

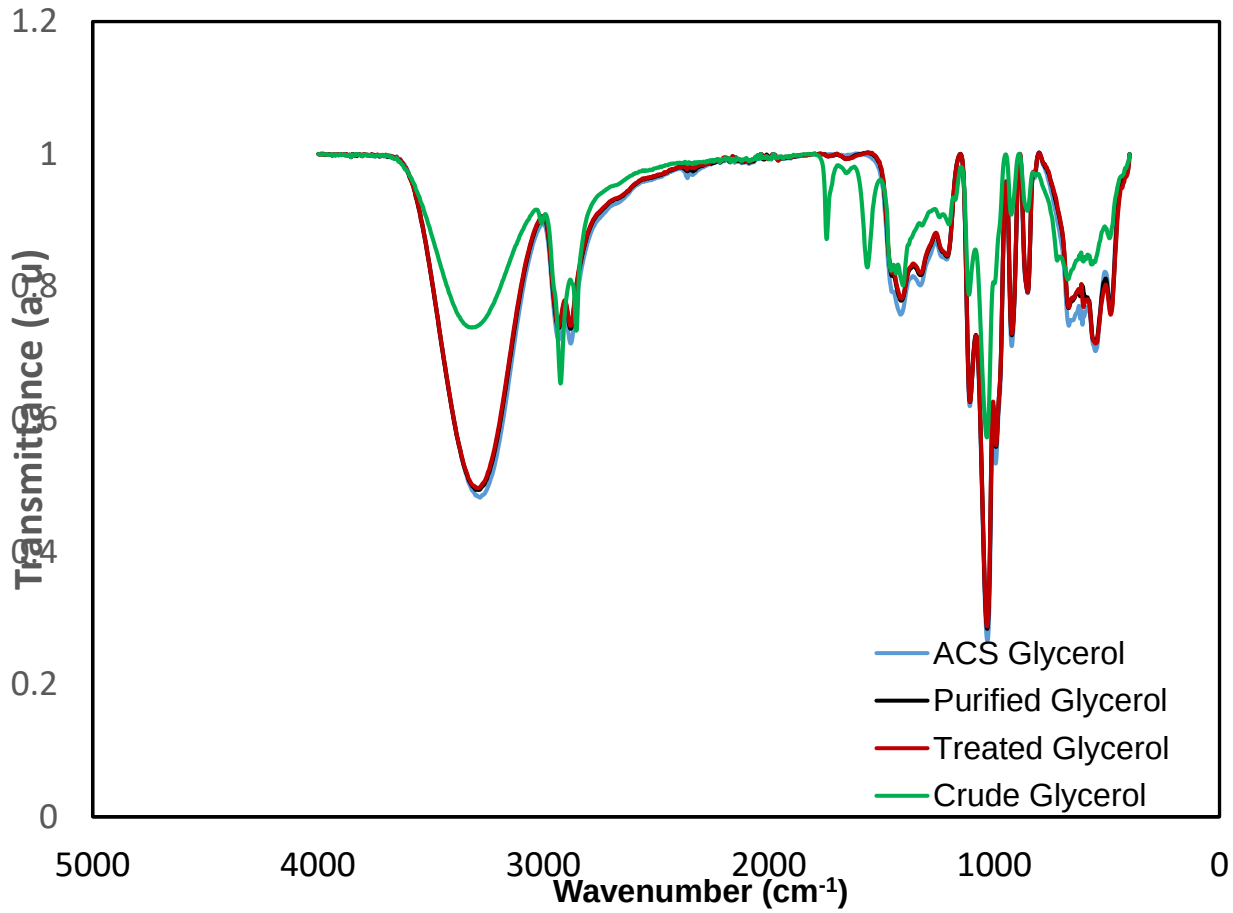

Figure 4-3 FTIR spectra for crude, enriched (treated step 1 and purified step 2) and ACS grade glycerol

From the spectra, it can be seen that ACS grade glycerol and enriched (treated and purified) glycerol have similar spectra as they almost map onto each other perfectly. Crude glycerol though has a distinctly different spectra from the rest due to its impurity content. A broad peak at 3200-3400 cm^{-1} present in all four glycerol samples is a characteristic peak due to –OH stretching (Dhabhai et al., 2016). This peak due to –OH stretching was low for crude glycerol. The following other functional groups were identified from resolved peaks at the said wavenumbers for all the four glycerol samples: O-H bending at 920 cm^{-1}, C-O stretching from 1100 cm^{-1} (more intense peak due to secondary alcohol) to 1450 cm^{-1} (primary alcohol), C-O-H bending at 1400 to 1460 cm^{-1}, H_2O blending at 1650cm^{-1} , C-H stretching at 2880 and 2930 cm^{-1} (more intense for glycerol),

and C-O stretching at 2100 cm^{-1} (Ooi et al., 2001). The spectra of the crude glycerol showed strong peaks at 1550-1580 and 1740 cm^{-1} and a small band at 3050 cm^{-1} which signaled the presence of a COO^- functional group suggesting the presence of esters or carboxylic acids of fatty acids or SFA. These peaks were completely absent in purified glycerol spectra. The small absorbance band at around 2900 cm^{-1} is due to the presence of unsaturated C=C functional group (Dhabhai et al., 2016; Kongjao et al, 2010).

4.4 Activated charcoal adsorption

Activated carbon adsorption was employed as a finishing step to further improve glycerol purity and to remove the color (Ardi et al., 2015). Organic compounds smaller than the pore sizes of activated carbon get absorbed between its pores (Ardi et al., 2015). Treatment with activated carbon generally removes residual fatty acids and colour (Ardi et al., 2015). However, as in the present case, all the FFA was removed in physicochemical treatment, with activated charcoal treatment, no significant improvement in glycerol purity was obtained. The only improvement was significant reduction in colour, as the enriched glycerol was colorless and resembled commercial grade glycerol in appearance (Ardi et al., 2015).

4.5 Techno-economic feasibility study and cash flow analysis

Economic evaluation refers to the evaluation of capital and operating costs associated with construction and operation of a chemical process (Turton et al., 1998). The criteria for economic evaluation in this work was based on capital cost, manufacturing cost and project profitability as measured by cumulative cash flows and net present value or worth (NPV/NPW) of the project.

Three different hypothetical scenarios were studied in this work. In scenario 1, all the purified glycerol was to be sold directly as it was. In Scenario 2, 50% of the purified glycerol was to be sold directly, while 50% was to be converted to value-added fuel additives – 25% to solketal, and

the other 25% to glycerol carbonate. In Scenario 3, all purified glycerol was to be converted to value-added fuel additives with 50% being converted to solketal and the other 50% into glycerol carbonate. The three scenarios were then compared on the basis of per unit cost of purifying glycerol and on per unit revenue generation ($/kg of crude glycerol). The details around cost determination used for tech-economic analysis are discussed in the following text.

4.5.1 Capital cost

Capital cost refers to the costs of constructing a new production plant or modifying an existing chemical plant. There are different types of capital cost estimates but the type used in this work is “Type 4” also known as “Study Estimate,” “Major Equipment Estimate” or “Factored Estimate” (Turton et al., 1998; Ulrich et al., 2004). In this work, the cost of major equipment and utilities were used to estimate the cost of building a grassroots project based on the experimental process. In the simulation of this work, the equipment were all auto-sized by Hysys based on process operating conditions, material and energy balances. The relevant equipment specification for the corresponding auto-sized equipment – power rating for pumps, surface area for heat exchangers, diameter, height and thickness for reactors, etc. - from Hysys were used along with the summary cost graphs to arrive at process equipment cost estimates (Ulrich et al., 2004).

The reactor type chosen in the simulation is conversion reactor for all the reactors used in the PFD. The cost of reactors was estimated based on the tables and graphs of process vessels, with the specialized vessels chosen to represent the reactors in cost estimation (Ulrich et al., 2004). Where heating was required, jacketed reactors were chosen (R-100 for saponification in the PFD in Appendix B). The heat exchangers chosen were floating head shell & tube exchanger type. For pumps, centrifugal radial types were chosen on the basis of the parameters of the required pump. To estimate the cost of separators, liquid cyclones were used to represent liquid-liquid separators for solvent extraction while sediment centrifuges were used to represent decanters (gravity

separators). Membranes and mixers were directly available in the cost graphs and were used to estimate the cost of the membrane separators and mixers used in the process respectively (Ulrich et al, 2004). Acidification reactor (R-101), gravity separator (V-100), heat exchanger (E-100), liquid-liquid separator (V-101) and neutralization reactor (R-102) and their piping systems were made of stainless steel (ss) because of the acidity of the crude glycerol solution at this point following acidification after saponification earlier. Most of the equipment used n the valorization of glycerol into fuel additives solketal and glycerol carbonate was also made of stainless steel as acids are used as reactants or in catalysts in these reactions.

Fixed capital cost, the total cost of equipment, has been calculated based on constructing a grassroots project since glycerol purification units would be added to a biodiesel plant that previously did not have glycerol purification equipment except basic equipment for separating crude glycerol from biodiesel. Fixed capital consists of bare module capital cost, contingencies & fees and auxiliary facilities costs (Olkiewicz et al., 2016). Total bare module cost is the sum of the equipment cost for all equipment used in a process (Ulrich et al., 2004). Contingencies and fees are based on total bare module capital cost and are calculated as a combined 18% (15% & 3% respectively) of the total bare module (Ulrich et al., 2004). Contingencies are meant to cover for any unforeseen circumstances while fees are for used to pay contractors' commission (Ulrich et al., 2004; Turton et al., 1998). Costs due to auxiliary facilities for a grassroots plant include land purchase, electrical & water system installation costs and costs of road and all internal constructions (Ulrich et al., 2004). Auxiliary costs constitute 30% of the total bare module capital (Ulrich et al., 2004). Total capital investment is calculated by adding a working capital to fixed capital (Ulrich et al., 2004). The former is estimated as a fraction of fixed capital cost and is usually taken as 15% of fixed capital cost (Ulrich et al., 2004).

4.5.2 Manufacturing cost

Manufacturing costs are defined as the costs associated with the day-to-day operation of a chemical plant or process. (Turton et al., 1998; Peter, 2015). To estimate manufacturing cost, process information from the PFD and an estimate of the fixed capital investment and the number of operators needed to operate the plant are required. The fixed capital investment is the same as either the total module cost or the grassroots (Reyniers et al., 2017; Ulrich et al., 2004). In this work, the fixed capital cost is equivalent to a grassroots cost of a project since the process in the current work is being built from scratch.

Manufacturing cost is composed of direct manufacturing costs, indirect (fixed) manufacturing costs and general expenses (Ulrich et al., 2004). Direct manufacturing costs represent operating expenses that vary with production rates and they consist of the costs of raw materials, catalysts and solvents, operating labor, supervision and clerical labour, utilities, maintenance and repairs, operating supplies, laboratory fees and patents and royalty fees (Olkiewicz et al., 2016; Ulrich et al., 2004).

Fixed or indirect manufacturing costs are independent of changes in production rates and include property taxes, insurance and depreciation (Peter, 2015; Ulrich et al., 2004). They are constant even when the plant is not in production (Ulrich et al., 2004). Indirect manufacturing costs include overhead costs, packaging, storage, insurance and depreciation fees and local taxes (Zhang et al., 2003).

General expenses represent an overhead burden necessary to carry out day-to-day business functions and include management, sales, financing and research functions (Zhang et al., 2003). General expenses rarely vary with production levels though research & development (R&D) and distribution & selling costs may decrease over extended periods of low production levels (Peter, 2015).

In this work, all the direct manufacturing costs for chemicals were calculated based on their individual prices (obtained from individual supplier websites and online current cost charts) and their flow rates or usage rate from the process simulation on Hysys (Appendices). The plant was assumed to run continuously 24 hours a day, and would employ 99 workers, assuming three workers for every two automated equipment, at a pay rate of $18.00/hr (~45,000 – 50,000/year) and three 8-hour shifts per day. There are a total of 22 major equipment that would require 33 operators per shift and there are three shifts hence 99 operators in total. The plant would consume 335.8 tons/year, which was calculated from an assumption of purification of 1 ton/day of crude glycerol on a 24 hour operating basis meaning three 8-hour shifts. The annual operating factor was assumed to be 0.92 throughout the year meaning 335.8 operating days per year. Based on an input of 1 ton/day of crude glycerol as raw material, the plant is expected to produce 134 tons/year of purified glycerol, some of which is converted to fuel additives such as solketal and glycerol carbonate or sold as pure glycerol. In this case, the plant glycerol yield is calculated as 97.3% wt% and purity is 94.2 wt%, all based on simulation results, which closely approximate experimental results. Glycerol makes up 40% of the input crude glycerol.

This is meant to be a small scale plant to begin with but should be expected to grow with more success. The plant operating hours are calculated to be 8059/year based on the 0.92 annual operating factor. All prices for raw materials and solvents and catalysts are assumed to be inclusive of other hidden costs. Utilities used in the current process are electricity, cooling water and hot oil. Other expenses such as supervisory and clerical labour fees, operating supplies charges and maintenance and repair expenses were estimated as a factor or fraction of the operating labour fees as is the case according to Ulrich's process engineering textbook (Zhang et al., 2003). At this early stage, most general expenses were set to zero as this is a small plant in the early stages of its

existence. Credits as a result of chemical recoveries (methanol, acetone and petroleum ether) were included in the calculation of manufacturing costs with unit cost sometimes being set as slightly less than that of buying a pure industrial grade chemical. Process total revenues were also considered and revenue per unit and cost per unit comparisons were made based on the three different scenarios considered. From the comparative manufacturing cost table for the three scenarios (Table 4-10), Scenario 1 has a unit cost of $7.12 per year and a unit revenue generation of $2.50. Scenario 2 costs $31.67 to purify and valorize a unit of crude glycerol and generates a revenue of $39.85 per unit of crude glycerol purified. Scenario 3 costs $50.45 per unit and generates $80.36 in per unit revenues.

On the basis of the above per unit cost and revenue, it is obvious that Scenario 3 is far and out the best option, clearly edging out Scenario 2. Scenario 1 results in net loss (cost: $7.12/unit, revenue: $2.58) and would never pay back the capital invested to start the project. Scenario 3 is therefore the easy choice assuming there is enough market for the solketal and glycerol carbonate that are produced from all the purified glycerol from the production process.

Table 4-10 presents the cost and revenue generation comparison of these three scenarios. As it can be seen, scenario 3 generated highest revenue compared to the other scenarios and also has higher profit margin per unit compared to scenario 2. Scenario 1 is outright unprofitable. It is also beneficial to opt for scenario 3 in regards to possible overproduction and environmental hazards of crude glycerol as it reduces glycerol availability in the market by having some of it valorized into fuel additives. This reduces overall crude and purified glycerol supply, as all of the purified glycerol is being utilized for value added chemical production. The details of cost determinants and comparative analysis of all three scenarios are presented as supplementary section in the Appendices.

Table 4-10 Comparative manufacturing costs and revenues tables for the three glycerol production scenarios

	Scenario 1		**Scenario 2**		**Scenario 3**	
Item	**Annual Cost ($)**	**Per Unit Annual Cost or Revenue ($/kg of crude glycerol)**	**Total Annual Cost**	**Per Unit Annual Cost ($/kg)**	**Total Annual Cost ($US)**	**Per Unit Annual Cost ($/kg)**
Direct manufacturing costs	664,728	4.75	3,720,230	27.70	6,133,284	45.66
Utilities	51,162	0.38	162,436	1.21	272,174	2.03
Indirect manufacturing costs	41,191	0.31	63,584	0.47	63,584	0.47
Maintenance & Repair (6% of fixed capital cost)	70,613	0.53	109,001	0.81	109,001	0.81
Operating supplies (15% of maintenance & repair)	10,592	0.08	16,350	0.12	16,350	0.12
Depreciation (10% of capital cost)	117,689	0.88	181,669	1.35	181,669	1.35
Total manufacturing expenses	**1,073,664**	**7.12**	**4,253,271**	**31.67**	**6,776,063**	**50.45**
Total annual revenues	**347,150**	**2.58**	**5,353,259**	**39.85**	**10,793,485**	**80.36**

4.5.3 Cash flow and Profitability analysis

In the cash flow analysis part of economic feasibility analysis, only the best case scenario (Scenario 3) was evaluated for profitability using a plot of cumulative cash flow against years of project life (Figure 4-4). These are the assumptions used in generating this cumulative cash flow chart. A fixed capital of $1.83M estimated based on equipment cost from PFD (Appendix B) and

working capital of $0.27M (15% of fixed capital) were invested in the project over a three year period during which there was no production. That is a total of $2.1M in total invested capital. After the first three years of capital investment, the project was to be operational for 10 years following start up at the beginning of year 4. Discounting interest rates of 10% and 15% were to be applied to project cumulative cash flow to determine final project NPV. Fixed capital was invested at a rate of $0.61M per year for the first three years with working capital also being invested in Year 3, making a total investment of $0.88M investment in Year 3 ($0.61M + $0.27M). Working capital ($0.27M) was to be recovered at the end of the project (Year 13 of total project life or year 10 of operation). Fixed capital was depreciated linearly at 10% over project life with zero salvage value at the end of project life. No allowances were considered and federal income tax was assumed to be 35%. During the first two years of project start-up (Years 4 and 5), revenues were assumed to be 80% of the projected amount ($8.63 M) while expenses were assumed to be 120% ($8.14 M) of what was to be projected. The normal projected revenues and expenses for later years (Years 6 through 13) were $10.73M and $6.78M respectively.

From Figure 4-4, it can be observed that the project payback period is just before year 6, which is how long it would take to recover the undiscounted fixed capital invested in the project. The project payback period is therefore just under three years after project start-up after year 3. The Discounted Break-even Period (DBEP) for the project would be 6.3 and 6.6 years (between years 6 and 7) for 10% and 15% discounting interest rates respectively as that is how long it would take for the discounted cumulative project capital to be recovered. So the net payout time (NPT) is 3.3 and 3.6 years for 10% and 15% discounting rates respectively. NPT is the point from project start-up (Year 3) to when cumulative cash flow becomes positive (between Years 6 and 7). The net present value (NPV) of the project is approximately $6 million and $3.65 million respectively at 10% and 15%

discounting interest rates since that is the final discounted cumulative cash flow amount at project conclusion.

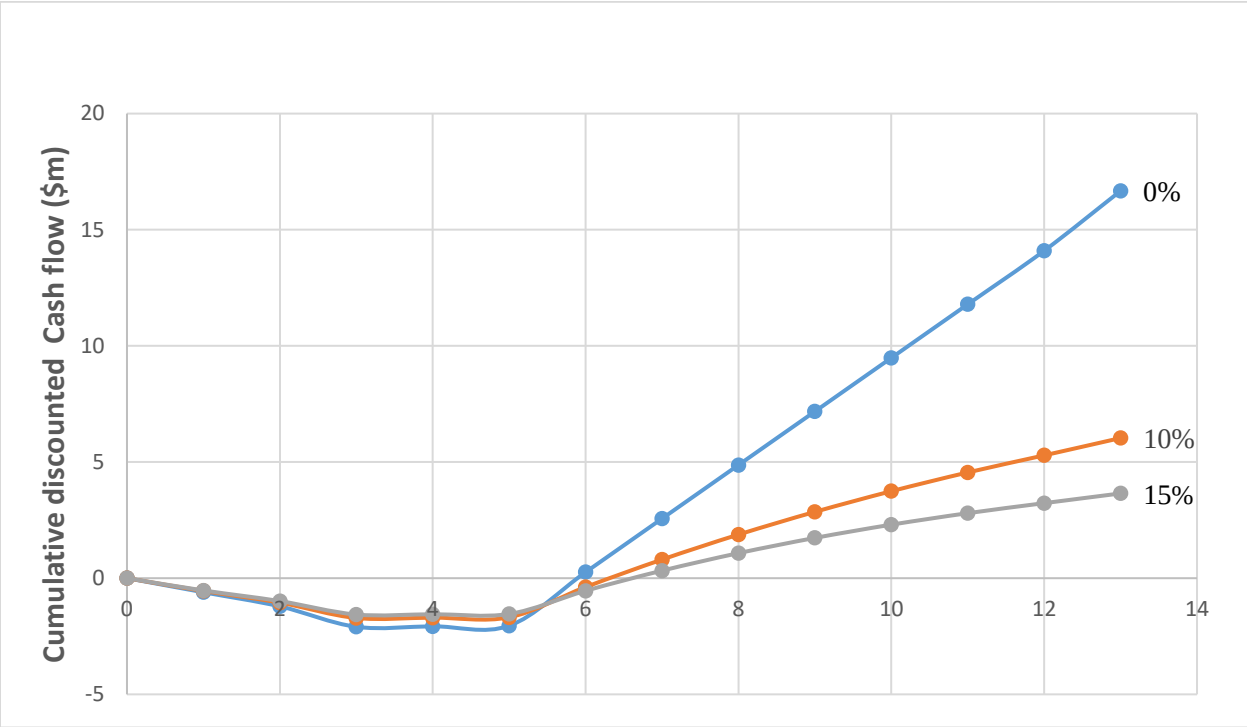

Figure 4-4 cumulative cash flow analysis at different discounting rates

Since this is an investment of just over $2 million in total capital input and expected discounted cumulative cash flow is $6 million at 10% discounting rate and $3.65 million at 15% discounting rate in net present value (NPV), this is a project worth undertaking as it promises to be profitable within 10 years after start-up. Capital investment has been assumed to take three years and revenues to be 80% and expenses to be 120% of what is to be expected in the first two years of project start-up (Years 4 and 5) before they become the normal projected amounts ($10.79 million in revenues and $6.78 million in expenses annually) until the end of project life 10 years

after start-up (Year 13). Per unit, annually, crude glycerol purification in this scenario costs $50.45 while it returns $80.36.

These are decent returns for a biodiesel plant as they will help offset production cost and increase profit margins. These returns indicate that it would be worth it investing in crude glycerol purification and valorization technology in addition to an existing biodiesel production plant. Another similar study for incorporation of glycerol purification plant in biodiesel production facility also suggested that it is beneficial to carry out glycerol purification after biodiesel production which will lead to revenue generation and reduction in wastewater treatment cost (Singhabhandhu et al., 2010).

5 CONCLUSIONS AND RECOMMENDATIONS

5.1 Conclusions

Crude glycerol was purified by combined physicochemical and semi-continuous tubular membrane filtration in this work. Physicochemical treatment comprising saponification, acidification, phase separation, and solvent extraction, removed most of the impurities such as FFA, glycerides, esters, and inorganics (as ash). The treatment enhanced glycerol purity to greater than 86 wt%. Further, membrane filtration of treated glycerol feed by ultrafiltration yielded the best glycerol purity results of 93.7 wt% obtained at 50°C temperature, 50 mL/min flow rate, and 690 kPa pressure with 95% yield for the process. These purity results are just under technical grade purity. Ultrafiltration membrane rejected large organics and colloidal particles from crude glycerol by sieving mechanism as per Darcy law, the operating law for ultrafiltration membrane filtration.

The combined effects of temperature, pressure and flow rate on the highest achievable glycerol purity during semi-continuous membrane filtration is best described by a two-factor interaction (2FI) model as determined by sum of squares and lack of fit tests methods from statistical analysis done on Design Expert 9 software. Adsorption using activated carbon as a finishing step improved glycerol purity further by adsorbing some organic macromolecules and removed color.

Nanofiltration studies done using simulated glycerol containing divalent salts showed a removal of 100% of divalent salts were rejected by it as glycerol purities of between 96 and 100 wt% were obtained from solutions of initial purities of 86.9 to 88.8 wt% with 4-5 wt% salt contents. Nanofiltration of treated glycerol was also performed and it gave the highest purity results of 97.2 and 94.9 wt% at 80 and 125 mL/min flow rates, both purities of which are of technical grade. A techno-economic analysis of the purification of glycerol by combined physico-chemical and optimized membrane ultrafiltration showed that the process is economically feasible when at least

50% of the purified glycerol is converted to value-added fuel additives such as solketal and glycerol carbonate but more profitable when all purified glycerol is valorized and sold as solketal and glycerol carbonate. A capital investment of $2.1 M over three years on a project that will be operational for 10 years after start-up resulted in $6.0 M or $3.65 M in net present value (NPV) at a 10% or 15% discounting rate in accordance with Scenario 3, where all the purified glycerol was converted to fuel additives solketal and glycerol carbonate. The unit annual general cost of Scenario 3 per kg of crude glycerol purified was found to be $50.45 while the unit revenue was projected to be $80.36.

5.2 Recommendations

Better and cheaper methods for water removal like the use of sodium thiosulfate on membrane purified glycerol are recommended as they can get glycerol purity to 98 wt% or higher. Scenario 3 is recommended along with crude glycerol purification by combined physico-chemical treatment and semi-continuous nanofiltration. In Scenario 3, all purified glycerol was to be converted to value-added fuel additives with 50% being converted to solketal and the other 50% into glycerol carbonate. It is recommended that the membrane filtration processes be made into continuous processes and run as such.

REFERENCES

Ahmad A.L., Mat Yasin NH, Derek CJC, Lim J.K. "Microalgae as a sustainable energy source for biodiesel production: a review." Renewable and Sustainable Energy Reviews Vol.15 (2011) 584–93.

Almena, A., M. Martin, "Technoeconomic Analysis of the Production of Epichlorohydrin from Glycerol," American Chemical Society (2015) A - M.

Alyson, S. F. Benny. "Fundamentals of Membranes for water treatment," University of Texas http://texaswater.tamu.edu/readings/desal/Membranetechnology.pdf

Apostolakou, A. A., I. K. Kookos, C. Marazioti, K. C. Angelopoulos, "Techno-economic Analysis of a Biodiesel Production Process from Vegetable Oils," Fuel Processing Technology, 90 (2009) 1023 - 1031.

Ardi, M. S., M. K. Aroua, N. A. Hashim, "Progress, Prospects and Challenges in Glycerol Purification Process: A Review," Renewable and Sustainable Energy Reviews, 42 (2015) 1164 - 1173.

Arora, A., B.S. Dien, R.L. Belyea, V. Singh, M.E. Tumbleson and K.D. Rausch, "Heat transfer fouling characteristics of microfiltered thin stillage from the dry grind process," Bioresource Technol., 101(16), 6521–6527 (2010).

Ashaghi, K. S., M. Ebrahimi, P. Czermak. "Ceramic ultra- and Nanofiltration membranes for oilfield produced water treatment: a mini review," Open Environmental Sciences Vol. 1 (2007) 1-8.

Atadashi, I.M., M.K. Aroua, A.R. Abdul Aziz, N.M.N. Sulaiman. "Crude biodiesel refining using membrane ultrafiltration process: An environmentally benign process," Egyptian Journal of Petroleum 24 (2015), 383 – 396.

Baker, R.W., "Membrane Technology and Applications," John Wiley & Sons, Ltd (2004).

Bjarne. N., “Developments in membrane technology for water treatment.” Desalination 2002; 153: 355-360.

Bohon, M. D., B. A. Metzger, W. P. Linak, C. J. King, W. L. Roberts. “Glycerol combustion and emissions. Proceedings of the Combustion Institute” 33 (2011) 2717–24.

Brouckaert, C.J., C.A. Buckley, E.P. Jacobs, “Common pitfalls in the design and operation of membrane plants – or how I should have done it,” Water Sci. Technol. 39(10–11), 107–114 (1999).

Cai, T, H. Li, H. Zhao, K. Liao, “Purification of crude glycerol from waste cooking oil based biodiesel production by orthogonal test method,” China Petroleum Processing and Petrochemical Technology, Vol. 15(1) (2013) 48-53.

Carmona, M., A. Lech, A. de Lucas, A. Perez, J. F. Rodriguez, “Purification of glycerol-water solutions from biodiesel synthesis by ion exchange: sodium and chloride removal,” Part II. J. Chem. Technol. Biotechnology 84 (2009) 1130−1135.

Cheryan, M., “Ultrafiltration and microfiltration handbook,” Technomic Publishing Co, Inc., Lancaster, Pennsylvania, USA, 1998.

Ciriminna, R., C. D. Pina, M. Rossi, M. Pagliaro, “Understanding the Glycerol Market,” European Journal of Lipid Science and Technology 116 (2014) 0000-0000.

Contreras-Andrade, I., E. Avella-Moreno, J. F. Sierra-Cantor, C. A. Guerrero-Fajardo, J. R. Sodre, “Purification of glycerol from biodiesel by sequential extraction monitored by 1H NMR,” Fuel Processing Technology 132 (2015) 99 – 104.

Cortinas, S., S. Luque, J.R. Alvarez, J. Canaval and J. Romero, “Microfiltration of kraft black liquor for the removal of colloidal suspended matter (pitch),” Desalination, 147, 49–54 (2002).

Da Silva, A. L., I. L. Müller. “Operation of solid oxide fuel cells on glycerol fuel: a thermodynamic analysis using the Gibbs free energy minimization approach,” Journal of Power Sources Vol. 195 (2010) 5637–44.

Dhabhai, R., E. Ahmadifeijani, A. K. Dalai, M. Reaney. “Purification of crude glycerol using a sequential physico-chemical treatment, membrane filtration, and activated charcoal adsorption,” Separation and Purification Technology, 168 (2016) 101-106.

Dow Chemical Company 2016 http://www.dow.com/optim/optimadvantage/physical-properties/viscosity.htm (assessed 10.02.16).

EET Corp. “Glycerol Purification.”, http://www.eetcorp.com/heepm/biodiesel.pdf

F. Schaffner, P.Y. Pontalier, V. Sanchez, F. Lutin, “Bipolar electrodialysis for glycerin production from diester wastes,” Filtra. Separ. 40 (2003) 35–39.

Fan, X. J., V. Urbain, Y. Qian, J. Manem, “Nitrification and mass balance with a membrane bioreactor for municipal wastewater treatment,” Water Sci. Technol. 34 (1996) 129–136.

Gerpen, J. V., B. Shanks, R. Pruszko, D. Clements, G. Knothe, “Biodiesel Production Technology,” National Renewable Energy Laboratory, Colorado, (2004) 1-105.

Guerrero-Perez, O. M., J. M. Rosas, J. Bedia, T. Cordero. “Recent inventions in glycerol transformations and processing,” Recent Patents on Chemical Engineering Vol. 2 (2009) 11–21.

Hajek, M., F. Skopal, “Treatment of glycerol phase formed by biodiesel production,” Bioresource Technology 101 (2010) 3242−3245.

He, Q., J. McNutt, J. Yang, “Utilization of the residual glycerol from biodiesel production for renewable energy generation,” Renewable and Sustainable Energy Reviews, 71 (2017) 63-76.

He, Q., J. McNutt, J. Yang. “Utilization of the residual glycerol from biodiesel production for renewable energy generation,” Renewable and Sustainable Energy Reviews 71 (2017) 63-76.

He, Y., Z.W. Jiang, “Technology review: treating oilfield wastewater,” Filtr. Sep. 45 (2008) 14–16.

Higgins, R. J., B. A. Bishop, R. L. Goldsmith. “Proceedings of the 3rd International Conference on Inorganic Membranes,” 1994 July, Worcester, MA; p. 447.

Holmqvist, A., O. Wallberg and A.-S. J¨onsson, Ultrafiltration of kraft black liquor from two Swedish pulp mills,” Chem. Eng. Res. Des., 83(A8), 994–999 (2005).

Horst H.C., J.M. Timmer, T. Robbertsen, J. Leenders, “Use of nanofiltration for concentration and demineralization in the dairy industry: Model for mass transport,” J. Membr. Sci. 104 (1995) 205.

Huang, H-W., S. Ramaswamy, W.W Al-Dajani, Tschirner U., 2010. “Process modeling and analysis of pulp mill-based integrated biorefinery with hemicelluloses pre-extraction for ethanol production:” A comparative study, Biores. Techn. 101, 624–631.

Huisman, H.L., “Cross-flow microflltration of particle suspensions: The influence of hydrodynamics and physicochemical interactions,” Thesis, Lund University, Sweden, 1988.

Hunsom, M., C. Autthanit. “Adsorptive purification of crude glycerol by sewage sludge-derived activated carbon prepared by chemical activation with H_3PO_4, K_2CO3 and KOH,” Chemical Engineering Journal 229 (2013) 334 – 343.

Hunsom, M., P. Saila, P. Chaiyakam, W. Kositnan, “Comparison and combination of solvent extraction and adsorption for crude glycerol enrichment,” International Journal of Renewable Energy Research, Vol. 3 (2) 2013.

Isahak, W. N. R. W., J. M. Jahim, M. Ismail, N. F. Nasir, M. M. Ba-Abbad, M. A. Yarmo. “Purification of crude glycerol from industrial waste: experimental and simulation studies,” Journal of Engineering Science and Technology 11 (8) 2016, 1056 – 1072.

Isahak, W. N. R. W., M. Ismail, M. A. Yarmo, J. M. Jahim, J. Salimon, "Purification of crude glycerol from transesterification RBD palm oil over homogeneous and heterogeneous catalysts for bio-lubricant preparation," J. App. Sci. 10 (21) (2010) 2590−2595.

Isahak, W.N.R.W., Z.A.C Ramli, M. Ismail, J.M. Jahim, M. A. Yarmo. "Recovery and purification of crude glycerol from vegetable oil transesterification, separation & purification reviews," 44 (3) (2015) 250 – 267 https://doi.org/10.1080/15422119.2013.851696

Javani, A., M. Hasheminejad, K. Tahvildari, M. Tabatabaei, "High quality potassium phosphate production through step-by-step glycerol purification: A strategy to economize biodiesel production," Bioresource Technology 104 (2012) 788 – 790.

Jeffrey, M., C. Yanwei, H. D. Robert. "Crossflow microfiltration of oily water," Journal of Membrane Science Vol. 129 (1997) 221-235.

Jonsson, A.S., and G. Tr¨ag˚ardh, Ultrafiltration Applications, Desalination, 77, 135–179 (1990).

Kirbawy S.A. and M.K. Hill, "Multivalent ion removal from kraft black liquor by ultrafiltration," Ind. Eng. Chem. Res., 26, 1851–1854 (1987).

Kongjao, S., S. Damronglerd, M. Hunsom, "Purification of crude glycerol derived from waste used-oil methyl ester plant," Korean J. Chem. Eng., 27 (3) (2010) 944-949.

Krawzcyk, H., and A.-S. Jonsson, "Separation of dispersed substances and galactoglucomannan in thermomechanical pulp waste water by microfiltration," Sep. Purif. Technol., 79, 43–49 (2011).

Le, N.L., S. P. Nunes, "Materials and membrane technologies for water and energy sustainability," Sustainable Materials and Technologies 7 (2016) 1-28.

Leberknight J., B. Wielenga, A. Lee-Jewett and T.J. Menkhaus, "Recovery of high value protein from a corn ethanol process by ultrafiltration and an exploration of the associated membrane fouling," J. Membrane Science, 366(1–2), 405–412 (2011).

Lee, H., G. Amy, J. Cho, Y. Yoon, S. H. Moon, I. S. Kim. “Cleaning strategies for cleaned flux ratio of an ultrafiltration membrane fouled by natural organic matter,” Water Res Vol. 35 (2001) 3301.

Lide. D..R.., ”Handbook of chemistry and physics,” 84th ed..Boca Raton: Fla.: CRC Press, Inc.; 1999.

Lipnizki, F., “Membrane process opportunities and challenges in the bioethanol industry,” Desalination, 250, 1067–1069 (2010).

Luo, X., X. Ge, S. Cui, Y. Li, “Value-added Processing of Crude Glycerol into Chemicals and Polymers,” Bioresource Technology, 215 (2016) 144 – 154.

Manosak, R., R. Limpattayanate, m. Hunsom, “Sequential refining of crude glycerol derived from waste used-oil methyl ester plant via a combined process of chemical and adsorption,” Fuel Process Technology 92 (2011) 92-99.

Manttari M., B. Van der Bruggen, M. Nystrom, “Nanofiltration: separation and purification technologies in Biorefineries,” 1st Ed., John Wiley & Sons Ltd., 2013.

McCoy, D., N. J. Mac. “Membrane Separation Technologies, Standard Handbook for Hazardous Waste Treatment and Disposal,” H.M. Freeman, ed., McGraw-Hill, New York: USA, 1988.

Miner, C.S., N. N. Dalton. “American chemical society, monograph series,” New York: Reinhold Publishing Company, 1953.

Morison, K.R., and X. She, “Optimisation and graphical representation of multi-stage membrane plants,” J. Membrane Science, 211, 59–70 (2003).

Morrison. L. R., “Glycerol,” Encyclopedia of Chemical Technology, New York: Wiley; 921–32.

Mulder. M., “Basic Principles of Membrane Technology,” Kluwer Academic Publishers, Dordrecht: The Netherlands, 1991.

Nanda, M. R., Z. Yuan, W. Qin, H. S. Ghaziaskar, M. Poirier, C. Xu. "Thermodynamic and kinetic studies of a catalytic process to convert glycerol into solketal as an oxygenated fuel additive," Fuel. Vol. 117 (2014) 470-477.

Nanda, M. R., Z. Yuan, W. Qiu, M. A. Poirier, X. Chunbao. "Purification of crude glycerol using acidification effects of acid types and product characterization," Austin Chemical Engineering 1(1) 2014.

Nordin, A.K., and A.-S. Jonsson, "Case study of an ultrafiltration plant treating bleach plant effluent from a pulp and paper mill," Desalination, 201, 277–289 (2006).

Okiel, K., Mona El-Sayed, Mohamed Y. El-Kady, "Treatment of oil–water emulsions by adsorption onto activated carbon, bentonite and deposited carbon," Egypt J. Petrol. 20 (2011) 9–15.

Olga Guerrero-Pérez, M., J.M. Rosas, J. Bedia, J. Rodríguez-Mirasol, T. Cordero, "Recent inventions in glycerol transformations and processing," Rec. Patents Chem. Eng. 2 (2009) 11-21.

Ooi, T. L., K. C. Yong, K. Dzulkefly, W. M. Z. Wan-Yunus, A. H. Hazimah, "Crude glycerine recovery from glycerol residue waste from a palm kernel oil methyl ester plant," J. of Oil Palm Research 13(2) (2001) 16-22.

Pagana, A., K. Stoitsas, V. T. Zaspalis. "Applied pilot-scale studies on ceramic membrane processes for the treatment of waste water streams," Global NEST J 2006; 8: 23-30.

Pagliaro, M., M. Rossi. "The Future of Glycerol," RSC Publishing, Cambridge: 2008.

Perry, M., C. Linder, "Intermediate reverse osmosis ultrafiltration (RO UF) membranes for concentration and desalting of low molecular weight organic solutes," Desalination 71 (1989) 233.

Peters. T., "Membrane Technology for Water Treatment," Chemical Engineering & Technology, 33 (8) 2010 1233-1240.

Peyravi, M., A. Rahimpour, M. Jahanshahi, “Developing nanocomposite PI membranes: Morphology and performance to glycerol removal at the downstream processing of biodiesel production,” Journal of Membrane Science 473 (2015) 72 – 84.

Posada, J. A., L. E. Rincon, C. A. Cardona, “Design and Analysis of Biorefineries based on Raw Glycerol: Addressing the Glycerol Problem,” Bioresource Technology, 111 (2012) 282 - 293.

Pott, R. W. M., C. J. Howe, J. S. Dennis, “The purification of crude glycerol derived from biodiesel manufacture and its use as a substrate by Rhodopseudomonas palustris to produce hydrogen,” Bioresource Technology 152 (2014) 464 – 470.

Potthast, R., Chung, C., Mathur, I., 2009. “Purification of glycerin obtained as a bioproduct from the transesterification of triglycerides in the synthesis of biofuel,” United States Patent, AC07C2980FI.

Puro, L., M. Kallioinen, M. M¨antt¨ari, G. Natarajan, C. Cameron and M. Nystr¨om, “Performance of RC and PES ultrafiltration membranes in filtration of pulp mill process waters,” Desalination, 264(3), 249–255 (2010).

Quispe, C.A.G., C. J.R. Coronado, J. A. Carvalho Jr. “Glycerol: production, consumption, prices, characterization and new trends in combustion,” Renewable and Sustainable Energy Reviews 27 (2013) 475 – 493.

Radiant Insights Inc., 2017 https://www.radiantinsights.com/press-release/global-glycerol-market

Rahmat, N., A.Z. Abdullah, A.R. Mohamed, “Recent progress on innovative and potential technologies for glycerol transformation into fuel additives: A critical review”, Renew. Sustain. Energy Rev., vol. 14, pp. 987-1000, April 2010.

Ramaswamy, S., Hua-Jiang, B. V. Ramarao. “Separation and Purification Technologies in Biorefineries,” 1st Ed., Publisher: John Wiley & Sons, Ltd., 2013.

Richard J, Ciora, Jr, Paul KT. “Liu Ceramic Membranes for Environmental Related Applications Fluid.” Particle Separation Journal 2003; 5: 51-60.

Sadhukhan, S., U. Sarkar, “Production of purified glycerol using sequential desalination and extraction of crude glycerol obtained during transesterification of Crotalaria juncea oil,” Energy Conversion and Management 118 (2016) 450 – 458

Saifuddin, N., H. Refal, P. Kumaran, “Rapid purification of glycerol by-product from biodiesel production through combined process of microwave-assisted acidification and adsorption via chitosan immobilized with yeast,” Research Journal of Applied Sciences, Engineering and Technology 7(3) 2014, 593 – 602.

Saleh, J., M. A. Dube, A. Y. Tremblay, “Separation of glycerol from FAME using ceramic membranes,” Fuel Processing Technology 92 (2011) 1305 – 1310.

Singh, R., “Membrane Technology and Engineering for Water Purification: Application, Systems Design and Operation,” 2nd Edition, Colorado Springs (2015), 1-200.

Singhabhandhu, A., T. Tezuka. “A perspective on incorporation of glycerin purification process in biodiesel plants using waste cooking oil as feedstock,” Energy, Vol. 35 (6) (2010), 2493-2504.

Soares, R. R., D. A. Simonetti, J. A. Dumesic. “Glycerol as a source for fuels and chemicals by low-temperature catalytic processing,” Angewandte Chemie 45 (24) (2006) 3982–5.

Sokker, H.H., Naeem M. El-Sawy, M.A. Hassan, Bahgat E. El-Anadouli, “Adsorption of crude oil from aqueous solution by hydrogel of chitosan based polyacrylamide prepared by radiation induced graft polymerization,” J. Hazard. Mater. 190 (2011) 359–365.

Spiegler K.S., Kedem O., 1966. “Thermodynamics of hyperfiltration (reverse osmosis): criteria for efficient membranes,” Desalination 1(4), 311–326.

Stelmachowski, M., “Utilization of glycerol, a by-product of the transesterification Process of vegetable oils: a review,” Ecological Chemistry and Engineering Vol. 18 (2011) 9–30.

Surrod, T., C. Pattamaprom, “Purification of glycerin by-product from biodiesel production using electrolysis process,” 2nd TSME International Conference on Mechanical Engineering (2011) 19-21.

Tan, H.W., A.R. Abdul Aziz, M.K. Aroua, “Glycerol production and its applications as a raw material: A review,” Renewable and Sustainable Energy Reviews, 27 (2013) 118-127.

Thompson, J. C., B. B. He. “Characterization of crude glycerol from biodiesel production from multiple feedstocks,” Applied Engineering in Agriculture Vol. 22 (2006) 261–5.

Turton, R., R. C. Baille, W. B. Whiting, J. A. Shaewitz. Toronto, CA: “Analysis, synthesis and design of chemical processes,” Prentice Hall International Series in the Physical and Chemical Engineering Sciences, 3rd Ed., 1998.

Ulrich, G., P. T. Vasude. Toronto, CA: “Chemical engineering process design and economics: a practical guide,” 2nd Ed., Process Publishing, 2004.

Vadthya, P., A. Kumari, C. Sumana, S. Sridhar, “Electrodialysis aided desalination of crude glycerol in the production of biodiesel from oil feed stock,” Desalination 362 (2015), 133 – 140

Valverde, J. L., A. de Lucas, M. Gonz´alez and J. F. Rodrıguez. “Equilibrium data for the exchange of Cu^{2+}, Cd^{2+}, and Zn^{2+} ions on the cationic exchanger Amberlite IR-120,” J Chem Eng Data (47) (2001) 613–617.

Van den Berg, G.B., I.G. Racz and C.A. Smolders, “Mass transfer coefficients in cross-flow ultrafiltration,” J. Membrane Sci., 47(1–2), 25–51 (1989).

Van der Bruggen B, Everaert K., Wilms D., Vandecasteele C., 2001. “Application of nanofiltration for removal of pesticides, nitrate and hardness from ground water: rejection properties and economic evaluation,” J. Membr. Sci. 193, 239–248.

Van Gerpen, J., B. Shanks, R. Pruszko, D. Clements, G. Knothe. “Subcontractor report, August 2002–January 2004,” Biodiesel Prod. Technol. (2004) 1-52

Van-der-Bruggen B., Van decasteele C. “Distillation vs. membrane filtration: overview of process evolutions in seawater desalination,” Desalination 2002; 143: 207-218.

Vigo, F., C. Uliana, E. Ravina, A. Lucifredi, M. Gandoglia. “The vibrating ultrafiltration module. Performance in the 50-1000 Hz frequency range,” Separation Science and Technology 28 (4) (1993) 1063-1076.

Vlysidis, A., M. Binns, C. Webb, C. Theodoropoulos, “A Techno-economic Analysis of Biodiesel Biorefineries: Assessment of Integrated Designs for the Co-Production of Fuels and Chemicals,” Energy, 36 (2011) 4671 - 4683.

Von Meien O. F., and R. Nobrega, “Ultrafiltration model for partial solute rejection in the limiting flux region,” J. Membrane Sci., 95, 277–287 (1994).

Wallberg, O., A.-S. J¨onsson and R. Wimmerstedt, “Fractionation and concentration of kraft black liquor with ultrafiltration,” Desalination, 154(2), 187–199 (2003).

Wang, K. Y., T. Chung. “The characterization of flat composite nanofiltration membranes and their applications in the separation of Cephalexin,” Journal of Membrane Science, Vol. 247 (2005) 37-50.

Wang, L. K., J. P. Chen, Y. Hung, N. K. Shammas, “Membrane and Desalination Technologies,” New York Handbook of Environmental Engineering, 13 (2011) 1-27.

Wang, Y., X. Wang, Y. Liu, S. Ou, Y. Tan, S. Tang, ”Refining of biodiesel by ceramic membrane separation,” Fuel Processing Technology 90 (2009) 422 – 427.

Werpy, T., G. Petersen, “Top value added chemicals from biomass, Results of Screening for Potential Candidates from Sugars and Synthesis Gas,” US DOE Report, vol. 1, (2004).

Xiao, Y., G. Xiao, A. Varma, “A Universal Procedure for Crude Glycerol Purification from Different Feedstocks in Biodiesel Production: Experimental and Simulation Study,” Industrial & Engineering Chemistry Research, 52 (2013) 14291 - 14296.

Yang, F., M. A. Hanna, R. Sun, “Value-added uses for crude glycerol – a by-product of biodiesel production,” Biotechnology for Biofuels (2012) 1-2.

Yong K.C., J., Ooi TL, Dzulkefly K, Wan Yunus WMZ, Hazimah AH. “Refining of crude glycerine recovered from glycerol residue by simple vacuum distillation.” Journal of Oil Palm Research 2001; 13:39–44.

Zabeti, M., W.M.A. M. K. Aroua, “Activity of solid catalysts for biodiesel production: a review,” Fuel processing Technology Vol. 90 (2009) 770-777.

Zajíc, J., 1988. Chemie a technologie tuku˚ . VŠCHT, Praha .

Zeitoun, R., P.Y. Pontalier, P. Marechal and L. Rigal, “Twin-screw extrusion for hemicellulose recovery: Influence on extract purity and purification performance,” Bioresource Technol., 101(23), 9348–9354 (2010).

Zhang, K., Y. Qin, F. He, J. Liu, Y. Zhang, L. Liu, “Concentration of aqueous glycerol solution by using continuous-effect membrane distillation,” Sep. Purif. Technol. 144 (2015) 186–196.

Zhang, Y., M. A. Dube, D. D. McLean, M. Kates. “Biodiesel production from waste cooking oil: 2. Economic assessment and sensitivity analysis,” Bioresources Technology 90 (2003) 229-240.

APPENDICES

Appendix A: Permission to Use Figures, Texts and Tables

Elsevier allows authors that publish articles with its journals to retain the copyright to include in their theses all or parts of their article(s) as long as they are not being republished for commercial purposes. With that right therefore, I have included in my Thesis most parts of my article published with Elsevier's Journal of Fuel Processing Technology. The said parts include parts of abstract, introduction, materials and methods, results and discussion, and conclusion and they comprise texts, tables and figures. The proof is attached below.

Copyright Clearance Center RightsLink®

Home | Create Account | Help

Title: Purification of crude glycerol derived from biodiesel production process: Experimental studies and techno-economic analyses

Author: Chol G. Chol,Ravi Dhabhai,Ajay K. Dalai,Martin Reaney

Publication: Fuel Processing Technology

Publisher: Elsevier

Date: September 2018

LOGIN

If you're a copyright.com user, you can login to RightsLink using your copyright.com credentials.

Already a RightsLink user or want to learn more?

Please note that, as the author of this Elsevier article, you retain the right to include it in a thesis or dissertation, provided it is not published commercially. Permission is not required, but please ensure that you reference the journal as the original source. For more information on this and on your other retained rights, please visit: https://www.elsevier.com/about/our-business/policies/copyright#Author-rights

BACK | CLOSE WINDOW

Appendix B: Process Flow Diagram

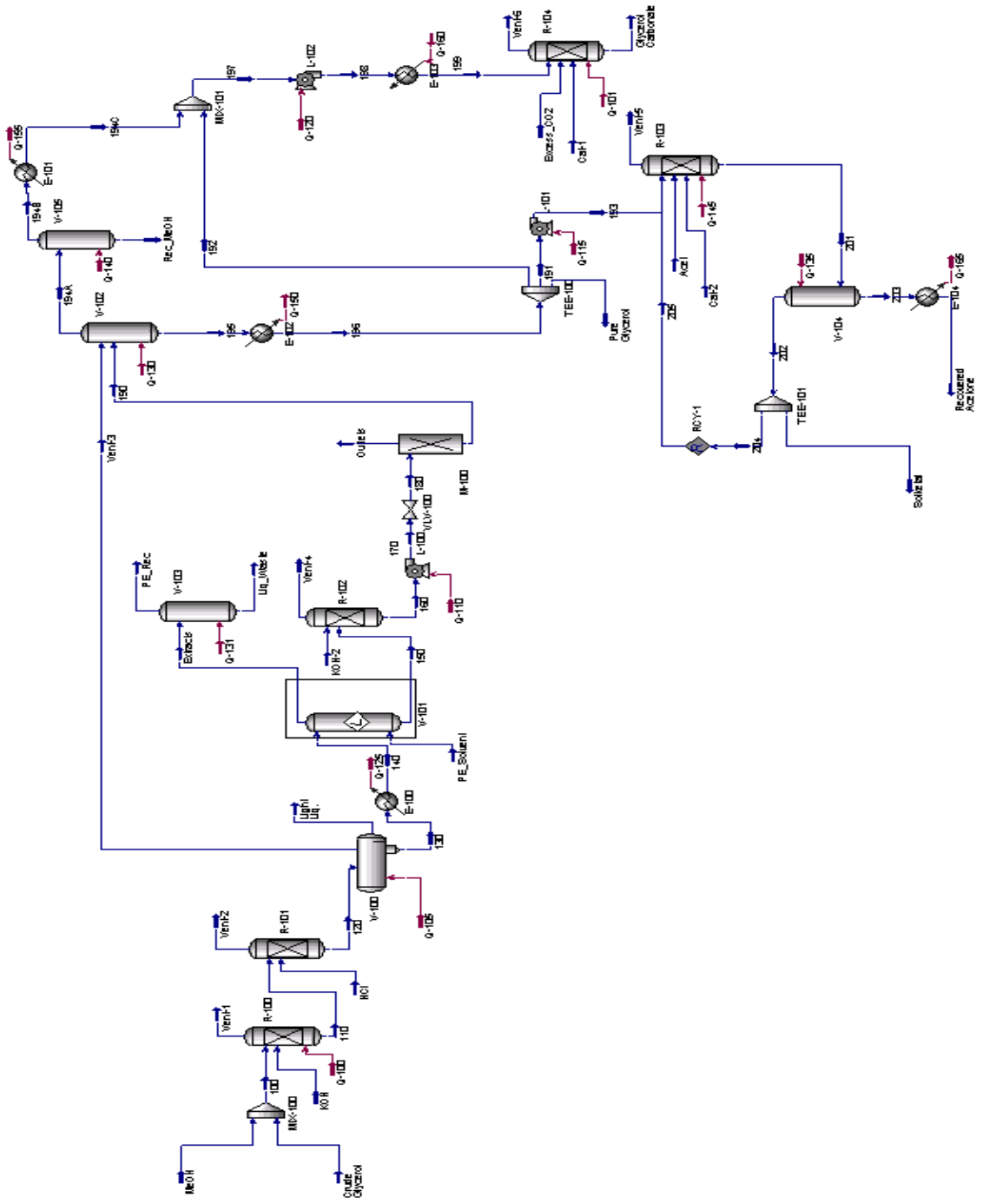

Figure B-1 Process flow diagram for techno-economic analysis

Chemical abbreviation [MeOH – methanol; Light Liq – light liquids; PE_solvent – petroleum ether solvent; PE_Rec – petroleum ether recovered; Liq_Waste – liquid waste; KOH and KOH-2 – potassium hydroxide; Cat-1 and Cat-2 – catalysts 1 and 2; Acet –acetone; Liq_Waste – liquid waste; Rec_MeOH – recovered methanol; Excess_CO2 – excess carbon dioxide].

Equipment abbreviation [MIX-100 and MIX-101 – mixers; R-100, R-101, R-102, R-103 and R-104 – conversion reactors for saponification, acidification, neutralization, ketalization and carboxylation, respectively; V-100 – gravity separator; E-100, E-101, E-102, E-103 and E-104 – heat exchangers; V-101 – liquid-liquid separator; V-102, V-103, V-104 – flash separators; L-100, L-101, L-102 – pumps; VLV-100 – feed control valve; M-100 – membrane separator; T-100 and T-101 – Tee-splitters; RCY-1 – recycle symbol; and Q-100, Q-105, Q-110, Q-115, Q-120, Q125, Q-130, Q-135, Q-140, Q-145, Q-150, Q-155, Q-160, Q-165, Q-170 – cooling or heating energy sources]

Appendix C: Assessment of Economic Scenarios for Glycerol Purification

Table C-1 Scenario 1: 100% glycerol product and zero value-added products

Item	**Annual Cost ($)**	**Per Unit Annual Cost or Revenue ($/Kg of crude glycerol)**
Direct manufacturing costs	664728	4.95
Utilities	51162	0.38
Indirect manufacturing costs	41191	0.31
Maintenance & Repair (6% of fixed capital cost)	70613	0.53
Operating supplies (15% of maintenance & repair)	10592	0.08
Depreciation (10% of capital cost)	117689	0.88
Total manufacturing expenses	**1073664**	**7.12**
Total annual revenues	**347150**	**2.58**

Appendix D: Scenario 2

Table D-1 50% pure glycerol product, 25% glycerol carbonate and 25% solketal

Item	**Annual Cost ($US)**	**Per Unit Cost or Revenue ($/Kg of crude glycerol)**
Direct manufacturing costs	3720230	27.70
Utilities	162436	1.21
Indirect manufacturing costs	63584	0.47
Maintenance & Repair (6% of fixed capital cost)	109001	0.81
Operating supplies (15% of maintenance & repair)	16350	0.12
Depreciation (10% of capital cost)	181669	1.35
Total manufacturing expenses	**4253271**	**31.67**
Total annual revenues	**5353259**	**39.85**

Appendix E: Scenario 3: 0% pure glycerol, 50% each converted into glycerol carbonate and solketal

Table E-1 Summary of manufacturing costs and revenues for Scenario 3

Expenses			**Daily Capacity (Kg, L, m3 (for wastes), persons)**	**Total Annual Cost ($/yr)**	**Cost/Unit product**
Direct	Raw materials	Crude glycerol	1000	0	0
		Methanol	816.48	1302326	9.70
		CO2	186.12	43749	0.33
	By-product credits	Acetone	306.00	68850	-11.48
		Methanol	859.44	-1370850	-10.21
		Petroleum ether	216.63	-872932	-6.50
	Catalysts & Solvents	KOH	3.41	1247	0.01
		HCl	3.14	7390	0.06
		Petroleum ether	335.28	1435485	10.69
		Acetone	874.80	4993883	37.18
		Amberlyst-15	7.89	10603	0.08
		Dibutyltin ether	16.28	1465469	10.91
	Operating labour	Workers	99	598396	4.46

	Supervisory & clerical labour (20% of operating labour)			59840	0.45
			Total Direct ME	6133284	45.66
Utilities	Electricity			231602	1.72
	Cooling water			34624	0.26
	Heating oil			5948	0.04
			Total Utility Cost	272174	2.03
Maintenance & Repair (6% of Cfc)				109001	0.81
Operating supplies (15% of maintenance & repair)				16350	0.12
	Total			**6530810**	**48.62**
Indirect					
	Local taxes (2% Cfc)			36334	0.27
	Insurance (1.5% Cfc)			27250	0.20
	Total			**63584**	**0.47**
Total Manufacturing Expense = DME + IME				**6594394**	**49.09**
Depreciation (10% Cfc)				181669	1.35
	Total expenses			**6776063**	**50.45**
Glycerol			0.00	0.00	0.00
Solketal			294.96	10399995	77.43

Glycerol carbonate			260.40	393490	2.93
Total Revenues				**10,793,485**	**80.36**

Appendix F: Cost and Revenue Table

Table F-1 Summary table for different aspects of project manufacturing costs and revenues for all the scenarios

	Scenario 1		**Scenario 2**		**Scenario 3**	
Item	**Total annual cost ($)**	**Annual cost and revenue ($/kg of crude glycerol)**	**Total annual cost ($)**	**Annual cost and revenue ($/kg of crude glycerol)**	**Annual Cost ($)**	**Per Unit Cost or Revenue ($/Kg of crude glycerol)**
Direct manufacturing costs	664,728	4.75	3,720,230.13	27.70	6,133,284	45.66
Utilities	51,162	0.38	162,435.96	1.21	272,174	2.03
Indirect manufacturing costs	41,191	0.31	63,584.18	0.47	63,584	0.47
Maintenance & Repair (6% of fixed capital cost)	70,613	0.53	109,001.44	0.81	109,001.44	0.81
Operating supplies (15% of maintenance & repair)	10,592	0.08	16,350	0.12	16,350	0.12
Depreciation (10% of capital cost)	117,689	0.88	181,669	1.35	181,669	1.35
Total manufacturing expenses	**1,073,664**	**7.12**	**4,253,271**	**31.67**	**6,776,063**	**50.45**
Total annual revenues	**347,150**	**2.58**	**5,353,259**	**39.85**	**10,793,485**	**80.36**

Appendix G: Cash flow (Profitability) Tables for Scenario 3

Table G-1 Undiscounted cash flows

Net Profit aft. Taxes	Federal Income Taxes	Net Profit bef. Taxes	Allowances	Depreciation	Annual Cash Income	Total Expenses (ex. Dep)	Sales Income	Annual Capital Investment	Year
0	**0**	**0**	**0**	**0**	**0**	**0**	**0**	-0.61	**1**
0	**0**	**0**	**0**	**0**	**0**	**0**	**0**	-0.61	2
0	**0**	**0**	**0**	**0**	**0**	**0**	**0**	-0.88	3
0.20	0.11	0.31	**0**	-0.18	0.50	8.14	8.63	0	4
0.20	0.11	0.31	**0**	-0.18	0.50	8.14	8.63	0	5
2.49	1.34	3.83	**0**	-0.18	4.01	6.78	10.79	0	6
2.49	1.34	3.83	**0**	-0.18	4.01	6.78	10.79	0	7
2.49	1.34	3.83	**0**	-0.18	4.01	6.78	10.79	0	8
2.49	1.34	3.83	**0**	-0.18	4.01	6.78	10.79	0	9
2.49	1.34	3.83	**0**	-0.18	4.01	6.78	10.79	0	10
2.49	1.34	3.83	**0**	-0.18	4.01	6.78	10.79	0	11
2.49	1.34	3.83	**0**	-0.18	4.01	6.78	10.79	0	12
2.49	1.34	3.83	**0**	-0.18	4.01	6.78	10.79	0.27	13

Net Cash Income	**-0.61**	**-0.61**	**-0.88**	**0.02**	**0.02**	**2.31**	**2.31**	**2.31**	**2.31**	**2.31**	**2.31**	**2.58**

Table G-2 Discounted cumulative cash flows at 0% (undiscounted), 10% and 15%

		0	0.10			0.15		
End of Year	**Annual**	**Cummulative**	**Discounting Factor**	**Annual**	**Cummulative**	**Discounting Factor**	**Annual**	**Cummulative**
1.00	-0.61	-0.61	0.91	-0.55	-0.55	0.87	-0.53	-0.53
2.00	-0.61	-1.21	0.83	-0.50	-1.05	0.76	-0.46	-0.99
3.00	-0.88	-2.09	0.75	-0.66	-1.71	0.66	-0.58	-1.56
4.00	0.02	-2.07	0.68	0.02	-1.70	0.57	0.01	-1.55
5.00	0.02	-2.05	0.62	0.01	-1.68	0.50	0.01	-1.54
6.00	2.31	0.26	0.56	1.30	-0.38	0.43	1.00	-0.54
7.00	2.31	2.56	0.51	1.18	0.80	0.38	0.87	0.32
8.00	2.31	4.87	0.47	1.08	1.88	0.33	0.75	1.08
9.00	2.31	7.18	0.42	0.98	2.86	0.28	0.66	1.73
10.00	2.31	9.48	0.39	0.89	3.74	0.25	0.57	2.30
11.00	2.31	11.79	0.35	0.81	4.55	0.21	0.50	2.80
12.00	2.31	14.10	0.32	0.73	5.29	0.19	0.43	3.23
13.00	2.58	16.67	0.29	0.75	6.03	0.16	0.42	3.65
Ending Value		**16.67**			**6.03**			**3.65**